

THEORY OF DIELECTRIC ELASTOMERS

Zhigang Suo *

*School of Engineering and Applied Sciences, Kavli Institute for Nanobio Science
and Technology, Harvard University, Cambridge, MA 02138*

ABSTRACT In response to a stimulus, a soft material deforms, and the deformation provides a function. We call such a material a soft active material (SAM). This review focuses on one class of soft active materials: dielectric elastomers. Subject to a voltage, a membrane of a dielectric elastomer reduces thickness and expands area, possibly straining over 100%. The phenomenon is being developed as transducers for broad applications, including soft robots, adaptive optics, Braille displays, and electric generators. This paper reviews the theory of dielectric elastomers, coupling large deformation and electric potential. The theory is developed within the framework of continuum mechanics and thermodynamics, and is motivated by molecular pictures and empirical observations. The theory is used to describe nonlinear and nonequilibrium behavior, such as electromechanical instability and viscoelasticity. It is hoped that the theory will aid in the creation of materials and devices.

* Email: suo@seas.harvard.edu

** The work reviewed here was carried out over the last six years, supported by NSF (CMMI-0800161, Large deformation and instability in soft active materials), by MURI (W911NF-04-1-0170, Design and Processing of Electret Structures; W911NF-09-1-0476, Innovative Design and Processing for Multi-Functional Adaptive Structural Materials), and by DARPA (W911NF-08-1-0143, Programmable Matter; W911NF-10-1-0113, Cephalopod-inspired Adaptive Photonic Systems).

This paper is submitted to a special issue of Acta Mechanica Solida Sinica on the occasion of its 30th anniversary.

| Report Documentation Page | | | Form Approved OMB No. 0704-0188 | |
|--|------------------------------------|--|---|---|
| Public reporting burden for the collection of information is estimated to average 1 hour per response, including the time for reviewing instructions, searching existing data sources, gathering and maintaining the data needed, and completing and reviewing the collection of information. Send comments regarding this burden estimate or any other aspect of this collection of information, including suggestions for reducing this burden, to Washington Headquarters Services, Directorate for Information Operations and Reports, 1215 Jefferson Davis Highway, Suite 1204, Arlington VA 22202-4302. Respondents should be aware that notwithstanding any other provision of law, no person shall be subject to a penalty for failing to comply with a collection of information if it does not display a currently valid OMB control number. | | | | |
| 1. REPORT DATE 25 OCT 2010 | | 2. REPORT TYPE | | 3. DATES COVERED 00-00-2010 to 00-00-2010 |
| 4. TITLE AND SUBTITLE Theory of Dielectric Elastomers | | 5a. CONTRACT NUMBER | | |
| | | 5b. GRANT NUMBER | | |
| | | 5c. PROGRAM ELEMENT NUMBER | | |
| 6. AUTHOR(S) | | 5d. PROJECT NUMBER | | |
| | | 5e. TASK NUMBER | | |
| | | 5f. WORK UNIT NUMBER | | |
| 7. PERFORMING ORGANIZATION NAME(S) AND ADDRESS(ES) Harvard University,School of Engineering and Applied Sciences,Kavli Institute for Nanobio Science and Technology,Cambridge,MA,02138 | | 8. PERFORMING ORGANIZATION REPORT NUMBER | | |
| 9. SPONSORING/MONITORING AGENCY NAME(S) AND ADDRESS(ES) | | 10. SPONSOR/MONITOR'S ACRONYM(S) | | |
| | | 11. SPONSOR/MONITOR'S REPORT NUMBER(S) | | |
| 12. DISTRIBUTION/AVAILABILITY STATEMENT Approved for public release; distribution unlimited | | | | |
| 13. SUPPLEMENTARY NOTES | | | | |
| 14. ABSTRACT In response to a stimulus, a soft material deforms, and the deformation provides a function. We call such a material a soft active material (SAM). This review focuses on one class of soft active materials: dielectric elastomers. Subject to a voltage, a membrane of a dielectric elastomer reduces thickness and expands area, possibly straining over 100%. The phenomenon is being developed as transducers for broad applications, including soft robots, adaptive optics, Braille displays, and electric generators. This paper reviews the theory of dielectric elastomers, coupling large deformation and electric potential. The theory is developed within the framework of continuum mechanics and thermodynamics, and is motivated by molecular pictures and empirical observations. The theory is used to describe nonlinear and nonequilibrium behavior, such as electromechanical instability and viscoelasticity. It is hoped that the theory will aid in the creation of materials and devices. | | | | |
| 15. SUBJECT TERMS | | | | |
| 16. SECURITY CLASSIFICATION OF: | | | 17. LIMITATION OF ABSTRACT Same as Report (SAR) | 18. NUMBER OF PAGES 55 |
| a. REPORT unclassified | b. ABSTRACT unclassified | c. THIS PAGE unclassified | | |

I. INTRODUCTION

1.1. Soft Active Materials for Soft Machines

The convergence of parts of biology and engineering has created exciting opportunities of discovery, invention and commercialization. The overarching themes include using engineering methods to advance biology, combining biology and engineering to invent medical procedures, and mimicking biology to create engineering devices.

Machines in engineering use mostly hard materials, while machines in nature are often soft. What does softness impart to the life of animals and plants? A conspicuous feature of life is to receive and process information from the environment, and then move. The movements are responsible for diverse functions, far beyond the function of going from place to place. For example, an octopus can change its color at an astonishing speed, for camouflage and signaling. This rapid change in color is mediated by thousands of pigment-containing sacs. Attach to the periphery of each sac are dozens of radial muscles. By contracting or relaxing the muscles, the sac increases or decreases in area in less than a second. An expanded sac may be up to about 1 mm in diameter, showing the color. A retracted sac may be down to about 0.1 mm in diameter, barely visible to the naked eye^[1].

As another example, in response to a change in the concentration of salt, a plant can change the rate of water flowing through the xylem. This regulation of flow is thought to be mediated by pectins, polysaccharides that are used to make jellies and jams. Pectins are long polymers, crosslinked into a network. The network can imbibe a large amount of water and swell many times its own volume, resulting in a hydrogel. The amount of swelling changes in response to a change in the concentration of salt. The change in the volume of the hydrogel alters the size of the microchannels in the xylem, regulating the rate of flow^[2].

The above examples are concerned with animals and plants. But many more examples are everywhere around and inside us. Consider the accommodation of the eye, the beating of the heart, the sound shaped by the vocal folds, and the sound in the ear. Abstracting these

biological soft machines, we may say that a stimulus causes a material to deform, and the deformation provides a function (Fig. 1). Connecting the stimulus and the function is the material capable of large deformation in response to a stimulus. We call such a material a soft active material (SAM).

An exciting field of engineering is emerging that uses soft active materials to create soft machines. Soft active materials in engineering are indeed apt in mimicking the salient feature of life: movements in response to stimuli. An electric field can cause an elastomer to stretch several times its length. A change in pH can cause a hydrogel to swell many times its volume. These soft active materials are being developed for diverse applications, including soft robots, adaptive optics, self-regulating fluidics, programmable haptic surfaces, and oilfield management^[3-8].

Research in soft active materials has once again brought mechanics to the forefront of human creativity. The familiar language finds new expressions, and deep thoughts are stimulated by new experience. To participate in advancing the field of soft active materials and soft machines effectively, mechanicians must retool our laboratories and our software, as well as adapt our theories.

The biological phenomena, as well as the tantalizing engineering applications, have motivated the development of theories of diverse soft active materials, including dielectric elastomers^[9-13], elastomeric gels^[14-19], polyelectrolytes^[20,21], pH-sensitive hydrogels^[22-24], and temperature sensitive hydrogels^[25]. The theories attempt to answer commonly asked questions. How do mechanics, chemistry, and electricity work together to generate large deformation? What characteristics of the materials optimize their functions? How do molecular processes affect macroscopic behavior? How efficiently can a material convert energy from one form to another? The theories are being implemented in software, so that they can become broadly useful in the creation of materials and devices.

1.2. Dielectric Elastomers

This review will focus on one particular class of soft active materials: dielectric elastomers. All materials contain electrons and ions—charged particles that move in response to an applied voltage. In a conductor, electrons or ions can move over a macroscopic distance. By contrast, in a dielectric, the charged particles move relative to one another by short distances. The two processes—deformation and polarization—are inherently coupled.

Fig.2 illustrates the principle of operation of a dielectric elastomer transducer. A membrane of a dielectric elastomer is sandwiched between two compliant electrodes. The electrodes have negligible electrical resistance and mechanical stiffness. A commonly used material for such electrodes is carbon crease. The dielectric is subject to forces and voltage. Charge flows through an external conducting wire from one electrode to the other. The charges of the opposite signs on the two electrodes cause the membrane to deform. It was discovered that an applied voltage may cause dielectric elastomers to strain over 100%^[3]. Because of this large strain, dielectric elastomers are often called artificial muscles. The discovery has inspired intense development of dielectric elastomers as transducers for diverse applications^[26-28].

This review focuses on the theory of dielectric elastomers. Section II describes the thermodynamics of a transducer of two independent variations. Emphasis is placed on basic ideas: states of the transducer, cyclic operation of the transducer, region of allowable states, equations of state, stability of a state, and nonconvex free-energy function. These ideas are described in both analytical and geometrical terms. Section III develops the theory of homogeneous fields. After setting up a thermodynamic framework for electromechanical coupling, we consider several specific material models: a vacuum as an elastic dielectric of vanishing rigidity, incompressible materials, ideal dielectric elastomers, and electrostrictive materials. Section IV applies nonequilibrium thermodynamics to dissipative processes, such as viscoelasticity, dielectric relaxation, and electrical conduction. Section V discusses electromechanical instability, both as a mode of failure and as a means to achieve giant voltage-

induced deformation. Section VI outlines the theory of inhomogeneous fields. A variational statement is formulated as the basis for the finite element method. The associated partial differential equations are summarized.

II. THERMODYNAMICS OF A TRANSDUCER

2.1. States of a Transducer

Fig. 3 illustrates a transducer, consisting of a dielectric separating two electrodes. The transducer is subject to a force P , represented by a weight. The two electrodes are connected through a conducting wire to a voltage Φ , represented by a battery. The weight moves by distance l , and the battery pumps charge Q from one electrode to the other.

The transducer is capable of two independent variations. Consequently, states of the transducer can be represented geometrically on a plane. The two coordinates of the plane may be chosen from variables such as P , Φ , l and Q . A point in the plane represents a state of the transducer. For example, Fig. 4 shows the force P and the displacement l as the coordinates of the plane. Plotted on the plane are the force-displacement curves of the transducer. Each force-displacement curve is measured under the condition that the two electrodes are subject to a constant voltage during deformation.

If the voltage between the electrodes can be varied, the force and the displacement may be changed independently. When the transducer is subject to a constant weight, but the voltage is changed from 0 to Φ_1 , the transducer changes from state A to state B, lifting the weight. When the displacement l is held constant, a change in the voltage causes the transducer to change from state A to state C, with accompanying change in the force.

We could have also plotted on the (l, P) plane curves of constant values of charge. Each curve of a constant charge is the force-displacement curve of the transducer measured under the open-circuit condition, when the two electrodes maintain a fixed amount of charge.

Following Gibbs's graphical method for a thermodynamic system of fluids^[29], we may choose any two of the four variables P , Φ , l and Q as coordinates. Each choice represents the transducer on a different plane. All these planes represent the same states of the transducer, because the transducer is capable only two independent variations. Nonetheless, different planes emphasize different attributes of the states. For example, the (P, Φ) plane may be used to indicate loading conditions, while the (l, Q) plane may be used to indicate kinematic conditions. The (l, Φ) plane is often used to report the voltage-induced deformation, while the (P, Q) plane may be used to report force-induced charge.

2.2. Cyclic Operations of a Transducer

Most applications involve cyclic changes of the state of the transducer. A particular cycle of states is illustrated in Fig. 5, on the (Q, Φ) plane. The voltage and the charge of the transducer can be changed independently. In changing from state A to state B, the transducer is connected to a battery of a low voltage, Φ_L ; a change in the applied force reduces the spacing between the two electrodes, causing the charge on the electrodes to increase. In changing from state B to state C, the transducer is under an open-circuit condition and the electrodes maintain the constant charge Q_H ; a change in the applied force increases the spacing between the two electrodes, raising the voltage to Φ_H . In changing from state C to state D, the transducer is connected to a battery of the high voltage Φ_H ; a change in the applied force increases the spacing between the two electrodes, causing the charge on the two electrodes to decrease. In changing from state D to state A, the transducer is under an open-circuit condition and the electrodes maintain the constant charge Q_L ; a change in the applied force decreases the spacing between the two electrodes, lowering the voltage to Φ_L .

The cycle receives mechanical work, and pumps charge from a low voltage to a high

voltage. Such a cycle describes a generator, harvesting electric energy by receiving mechanical work from the environment, such as the work done by an animal or human during walking, and the work done by ocean waves.

Indeed, a closed curve of any shape on the (Q, Φ) plane represents a cyclic operation of the transducer. The amount of energy converted per cycle is given by the area of the cycle on the (Q, Φ) plane. When the states cycle counterclockwise on the (Q, Φ) plane, the transducer is a generator, converting mechanical energy to electrical energy. When the states cycle clockwise on the (Q, Φ) plane, the transducer is an actuator, converting electrical energy to mechanical energy. The (l, P) plane can also be used to evaluate energy of conversion per cycle.

2.3. Modes of Failure and Region of Allowable States

A transducer may fail in multiple modes, such as mechanical rupture, electrical breakdown, electromechanical instability, and loss of tension^[30-32]. The critical condition for each mode of failure can be represented on the (Q, Φ) plane by a curve. Curves of all modes of failure bound in the plane a region, which we call the region of allowable states of the transducer. Such graphic methods have been used to optimize actuators^[33,34] and calculate the maximal energy of conversion for generators^[35-37]. Fig. 6 shows an example^[35].

2.4. Equations of State

On dropping a small distance δl , the weight does work $P\delta l$. On pumping a small amount of charge δQ , the battery does work $\Phi\delta Q$. The force is work-conjugate to the displacement, and the voltage is work-conjugate to the charge. We will analyze isothermal processes, and remove temperature from explicit consideration. Denote the Helmholtz free energy of the transducer by F . When the transducer equilibrates under the applied force and the applied voltage, the change in the free energy of the transducer equals the sum of the work

done by the weight and the work done by the battery:

$$\delta F = P\delta l + \Phi\delta Q. \quad (1)$$

This condition of equilibrium holds for arbitrary small variations δl and δQ . The displacement and the charge are independent variables.

The two independent variables (l, Q) characterize the state of the transducer. The Helmholtz free energy of the transducer is a function of the two independent variables:

$$F = F(l, Q). \quad (2)$$

Associated with small variations δl and δQ , the free energy varies by

$$\delta F = \frac{\partial F(l, Q)}{\partial l} \delta l + \frac{\partial F(l, Q)}{\partial Q} \delta Q. \quad (3)$$

A comparison of (1) and (3) gives

$$\left[\frac{\partial F(l, Q)}{\partial l} - P \right] \delta l + \left[\frac{\partial F(l, Q)}{\partial Q} - \Phi \right] \delta Q = 0. \quad (4)$$

When the transducer equilibrates with the weight and the battery, the condition of equilibrium (4) holds for independent and arbitrary variations δl and δQ . Consequently, in equilibrium, the coefficients of the two variations in (4) both vanish, giving

$$P = \frac{\partial F(l, Q)}{\partial l}, \quad (5)$$

$$\Phi = \frac{\partial F(l, Q)}{\partial Q}. \quad (6)$$

Once the free-energy function $F(l, Q)$ is known, (5) and (6) express P and Φ as functions of l and Q . That is, the two equations give the force and voltage needed to cause a certain displacement and a certain charge. The two equations (5) and (6) constitute the equations of state of the transducer.

Equation (5) can be used to determine the free-energy function from the force-displacement curves of the transducer measured under the open-circuit conditions, when the

electrodes maintain constant charges. For each value of Q , the free energy is the area under the force-displacement curve. Similarly, (6) can be used to determine the free-energy function from the voltage-charge curves of the transducer. As mentioned before, (l, P) and (Q, Φ) are convenient planes to represent the states of the transducer when we wish to highlight work and energy.

As an illustration, consider a parallel-plate capacitor—two plates of electrodes separated by a thin layer of a vacuum (Fig. 7). The separation l between the two electrodes may vary, but the area A of either electrode remains fixed. Recall the elementary fact that the amount of charge on either electrode is linear in the voltage:

$$\Phi = \frac{lQ}{\epsilon_0 A}, \quad (7)$$

where ϵ_0 the permittivity of the vacuum. Inserting (7) into (6) and integrating, we obtain the free-energy function

$$F(l, Q) = \frac{lQ^2}{2\epsilon_0 A}. \quad (8)$$

Inserting (8) into (5), we obtain that

$$P = \frac{Q^2}{2A\epsilon_0}. \quad (9)$$

Equations (7) and (9) constitute the equations of state of the parallel-plate capacitor. They are readily interpreted. The applied voltage causes charge to flow from one electrode to the other, so that one electrode is positively charged, and the other is negatively charged. Equation (7) relates the charge to the applied voltage. The oppositely charged electrodes attract each other. To maintain equilibrium, a force need be applied to the electrode. Equation (9) relates the applied force to the charge.

Define the electric field by $E = \Phi / l$ and the stress by $\sigma = P / A$. Rewrite (9) as

$$\sigma = \frac{1}{2} \epsilon_0 E^2. \quad (10)$$

This equation gives the stress needed to be applied to the electrodes to counteract the electrostatic attraction. This stress is known as the Maxwell stress.

2.5. Stability of a State

The equations of state, (5) and (6), are in general nonlinear. If the transducer operates in the neighborhood of a particular state (l, Q) , the equations of state can be linearized and written in an incremental form:

$$\delta P = \frac{\partial^2 F(l, Q)}{\partial l^2} \delta l + \frac{\partial^2 F(l, Q)}{\partial l \partial Q} \delta Q, \quad (11)$$

$$\delta \Phi = \frac{\partial^2 F(l, Q)}{\partial Q \partial l} \delta l + \frac{\partial^2 F(l, Q)}{\partial Q^2} \delta Q. \quad (12)$$

We call $\partial^2 F(l, Q)/\partial l^2$ the mechanical tangent stiffness of the transducer, and $\partial^2 F(l, Q)/\partial Q^2$ the electrical tangent stiffness of the transducer. The two electromechanical coupling effects are both characterized by the same cross derivative, $\partial^2 F(l, Q)/\partial l \partial Q = \partial^2 F(l, Q)/\partial Q \partial l$. Consequently, the two electromechanical coupling effects reciprocate. The matrix

$$\mathbf{H}(l, Q) = \begin{bmatrix} \frac{\partial^2 F(l, Q)}{\partial l^2} & \frac{\partial^2 F(l, Q)}{\partial l \partial Q} \\ \frac{\partial^2 F(l, Q)}{\partial l \partial Q} & \frac{\partial^2 F(l, Q)}{\partial Q^2} \end{bmatrix} \quad (13)$$

is known as the Hessian of the free-energy function $F(l, Q)$.

As mentioned above, a state of the transducer can be represented by a point in the (l, Q) , as well as by a point in the (P, Φ) plane. For the same state of the transducer, the point in the (l, Q) plane is mapped to the point in the (P, Φ) plane by the equations of state, (5) and (6). The mapping may not always be invertible. That is, given a pair of the loads (P, Φ) , the equations of

state may not be invertible to determine a state (l, Q) . For example, (11) and (12) are not invertible when the Hessian is a singular matrix, $\det \mathbf{H} = 0$. This singularity may be understood in terms of thermodynamics.

The transducer and the loading mechanisms (i.e., the weight and the battery) together constitute a thermodynamic system. The free energy of the system is the sum of the free energies of the individual parts—the transducer, the weight, and the battery. The free energy (i.e., the potential energy) of a constant weight is $-Pl$. The free energy of a battery of a constant voltage is $-\Phi Q$. Consequently, the free energy of the thermodynamic system combining the transducer and the loading mechanisms is

$$G(l, Q) = F(l, Q) - Pl - \Phi Q. \quad (14)$$

The system has two independent variables, l and Q .

Thermodynamics requires that the system should reach a stable state of equilibrium when the free-energy function $G(l, Q)$ is a minimum against small changes in l and Q . When the weight moves by δl and the battery pumps charges δQ , the free energy of the system varies by

$$\begin{aligned} \delta G = & \left[\frac{\partial F(l, Q)}{\partial l} - P \right] \delta l + \left[\frac{\partial F(l, Q)}{\partial Q} - \Phi \right] \delta Q \\ & + \frac{\partial^2 F(l, Q)}{2\partial l^2} (\delta l)^2 + \frac{\partial^2 F(l, Q)}{\partial l \partial Q} (\delta l)(\delta Q) + \frac{\partial^2 F(l, Q)}{2\partial Q^2} (\delta Q)^2 \end{aligned} \quad (15)$$

We have expanded the Taylor series up to terms quadratic in δl and δQ . In a state of equilibrium, the coefficients of the first-order variations vanish, recovering the equations of state (5) and (6). To ensure that this state of equilibrium minimizes G , the sum of the second-order variations must be positive for arbitrary combination of δl and δQ . That is, a state of equilibrium is stable if the Hessian of the free energy of the transducer, $\mathbf{H}(l, Q)$, is positive-definite. The two-by-two matrix is positive-definite if and only if

$$\frac{\partial^2 F(l, Q)}{\partial l^2} > 0, \quad \frac{\partial^2 F(l, Q)}{\partial Q^2} > 0, \quad \left[\frac{\partial^2 F(l, Q)}{\partial l^2} \right] \left[\frac{\partial^2 F(l, Q)}{\partial Q^2} \right] > \left[\frac{\partial^2 F(l, Q)}{\partial l \partial Q} \right]^2. \quad (16)$$

When the Hessian of the free energy function is positive-definite, the function $F(l, Q)$ is convex at this state (l, Q) .

As an illustration, consider the parallel-plate capacitor again. Given the free-energy function (8), the second derivatives are

$$\frac{\partial^2 F(l, Q)}{\partial l^2} = 0, \quad \frac{\partial^2 F(l, Q)}{\partial Q^2} = \frac{l}{\epsilon_0 A}, \quad \left[\frac{\partial^2 F(l, Q)}{\partial l \partial Q} \right] = \frac{Q}{\epsilon_0 A}. \quad (17)$$

Consequently, the Hessian is not positive-definite at any state of equilibrium. That is, the parallel-plate capacitor subject to a constant force and a constant voltage cannot reach a stable state of equilibrium. The conclusion is readily understood. The weight is independent of the separation between the plates, but the electrostatic attractive force increases as the separation decreases. Subject to a fixed weight, the two plates will be pulled apart if the voltage is small, and will be pulled together if the voltage is small.

The capacitor can be stabilized by a modification of the loading mechanisms. For example, we can replace the weight with a spring that restrains the relative movement of the plates. Let K be the stiffness of the spring, and l_0 be the separation between the electrodes when the spring is unstretched, so that the force in the spring is $P = K(l_0 - l)$. The free energy of the system is the sum of the free energies of the capacitor, the spring and the battery:

$$G(l, Q) = \frac{lQ^2}{2\epsilon_0 A} + \frac{1}{2} K(l - l_0)^2 - \Phi Q. \quad (18)$$

In a state of equilibrium, the first derivatives of $G(l, Q)$ vanish, giving the same equations of state as (10) and (12). The state of equilibrium is stable if and only if the Hessian of $G(l, Q)$ is positive-definite. The second derivatives of the function $G(l, Q)$ are

$$\frac{\partial^2 G(l, Q)}{\partial l^2} = K, \quad \frac{\partial^2 G(l, Q)}{\partial Q^2} = \frac{l}{\epsilon_0 A}, \quad \frac{\partial^2 G(l, Q)}{\partial l \partial Q} = \frac{Q}{\epsilon_0 A}. \quad (19)$$

A state of equilibrium (l, Q) is stable if and only if

$$\frac{Kl}{\epsilon_0 A} > \left(\frac{Q}{\epsilon_0 A} \right)^2. \quad (20)$$

Thus, the transducer is stable when the applied voltage is sufficiently small.

2.6. Nonconvex Free-Energy Surface

Following Gibbs^[38], we may interpret above analytical statements geometrically. Consider a three-dimensional space with (l, Q) as the horizontal plane, and F as the vertical axis. In this space, the Helmholtz free energy $F(l, Q)$ is represented by a surface. A pair of the loads (P, Φ) is represented by an inclined plane passing through the origin of the space, with P as the slope with respect to the l axis, and Φ the slope of the tangent plane with respect to the Q axis. By definition (14), the function $G(l, Q)$ is the vertical distance between the Helmholtz free energy surface and the inclined plane. Thermodynamics dictates that this vertical distance $G(l, Q)$ should minimize when the transducer equilibrates with the loads.

When the loads (P, Φ) are given, we may picture a plane simultaneously parallel to the inclined plane and tangent to the free-energy surface $F(l, Q)$. That is, the slope of the tangent plane with respect to the l axis is P , and the slope of the tangent plane with respect to the Q axis represents is Φ . From the geometry, it is evident that the state (l, Q) of the tangent point minimizes the vertical distance $G(l, Q)$. Also evident from the geometry, $G(l, Q)$ is minimum only if the free-energy surface $F(l, Q)$ in the neighborhood of the state (l, Q) is above the tangent plane—that is, the surface $F(l, Q)$ is convex at the state (l, Q) .

When the loads (P, Φ) change gradually, so are the slopes of the inclined plane. Consequently, as the loads (P, Φ) change gradually, the associated tangent plane rolls along the free-energy surface. If the free-energy surface $F(l, Q)$ is globally convex, every tangent plane touches the surface at only one point, and only one state (l, Q) is associated with a pair of given

loads (\mathbf{P}, Φ) . By contrast, if part of the free-energy surface $F(\mathbf{l}, \mathbf{Q})$ is concave, a tangent plane may touch the surface at two points, and two states (\mathbf{l}, \mathbf{Q}) are associated with a pair of given loads (\mathbf{P}, Φ) .

It was discovered that the free energy functions for dielectric elastomers are typically nonconvex^[39]. Associated with a given set of loads, more than one states of equilibrium may exist. The practical significance of nonconvex free-energy functions will be discussed later in connection with electromechanical instability.

III. HOMOGENEOUS FIELD

We now develop a field theory of deformable dielectrics. The field theory assumes that a material is a sum of many small pieces, and the field in each small piece is homogeneous. This assumption enables us to define quantities per unit length, per unit area, and per unit volume. This section focuses on the homogeneous field of a small piece, and Section VI considers inhomogeneous field of a body by summing up small pieces.

This section begins by setting up a thermodynamic framework for electromechanical coupling. We then consider several specific material models: a vacuum as an elastic dielectric of vanishing rigidity, incompressible materials, ideal dielectric elastomers, and electrostrictive materials.

3.1. Equations of State

With reference to Fig. 2, consider a block of an elastic dielectric, sandwiched between two compliant electrodes. In the reference state, the dielectric is subject to no forces and voltage, and is of dimensions L_1 , L_2 and L_3 . In the current state, the dielectric is subject to forces P_1 , P_2 and P_3 , and the two electrodes are connected to a battery of voltage Φ through a conducting wire. In the current state, the dimensions of the dielectric become l_1 , l_2 and l_3 , the

two electrodes accumulate electric charges $\pm Q$, and the Helmholtz free energy of the membrane is F .

When the dimensions of the dielectric change by δl_1 , δl_2 and δl_3 , the forces do work $P_1\delta l_1 + P_2\delta l_2 + P_3\delta l_3$. When a small quantity of charge δQ flows through the conducting wire, the voltage does work $\Phi\delta Q$. When the dielectric equilibrates with the forces and the voltage, the increase in the free energy equals the work done:

$$\delta F = P_1\delta l_1 + P_2\delta l_2 + P_3\delta l_3 + \Phi\delta Q. \quad (21)$$

The condition of equilibrium (21) holds for arbitrary small variations of the four independent variables, l_1 , l_2 , l_3 and Q .

Define stretches by $\lambda_1 = l_1/L_1$, $\lambda_2 = l_2/L_2$ and $\lambda_3 = l_3/L_3$, nominal stresses by $s_1 = P_1/(L_2L_3)$, $s_2 = P_2/(L_1L_3)$ and $s_3 = P_3/(L_1L_2)$, nominal electric field by $\tilde{E} = \Phi/L_3$, nominal electric displacement by $\tilde{D} = Q/(L_1L_2)$, and nominal density of the Helmholtz free energy by $W = F/(L_1L_2L_3)$. Also define true stresses by $\sigma_1 = P_1/(l_2l_3)$, $\sigma_2 = P_2/(l_1l_3)$ and $\sigma_3 = P_3/(l_1l_2)$, true electric field by $E = \Phi/l_3$, and true electric displacement by $D = Q/(l_1l_2)$.

The condition of equilibrium (21) holds in any current state. However, it is convenient to divide both sides of (21) by $L_1L_2L_3$, the volume of the block in the reference state. We obtain that

$$\delta W = s_1\delta\lambda_1 + s_2\delta\lambda_2 + s_3\delta\lambda_3 + \tilde{E}\delta\tilde{D}. \quad (22)$$

The condition of equilibrium holds for arbitrary small variations of the four independent variables, λ_1 , λ_2 , λ_3 and \tilde{D} .

As a material model, the nominal density of the Helmholtz free energy is prescribed as a function of the four independent variables:

$$W = W(\lambda_1, \lambda_2, \lambda_3, \tilde{D}). \quad (23)$$

Inserting (23) into (22), we obtain that

$$\left(\frac{\partial W}{\partial \lambda_1} - s_1\right)\delta\lambda_1 + \left(\frac{\partial W}{\partial \lambda_2} - s_2\right)\delta\lambda_2 + \left(\frac{\partial W}{\partial \lambda_3} - s_3\right)\delta\lambda_3 + \left(\frac{\partial W}{\partial \tilde{D}} - \tilde{E}\right)\delta\tilde{D} = 0. \quad (24)$$

This condition of equilibrium holds for any small variations of the four independent variables. Consequently, when the dielectric is in equilibrium with the applied forces and the applied voltage, the coefficient in front of the variation of each independent variable vanishes, giving

$$s_1 = \frac{\partial W(\lambda_1, \lambda_2, \lambda_3, \tilde{D})}{\partial \lambda_1}, \quad (25)$$

$$s_2 = \frac{\partial W(\lambda_1, \lambda_2, \lambda_3, \tilde{D})}{\partial \lambda_2}, \quad (26)$$

$$s_3 = \frac{\partial W(\lambda_1, \lambda_2, \lambda_3, \tilde{D})}{\partial \lambda_3}, \quad (27)$$

$$\tilde{E} = \frac{\partial W(\lambda_1, \lambda_2, \lambda_3, \tilde{D})}{\partial \tilde{D}}. \quad (28)$$

Equations (25)-(28) constitute yet another representation of the condition of equilibrium—they are called the equations of state. Once the free-energy function $W(\lambda_1, \lambda_2, \lambda_3, \tilde{D})$ is prescribed as a material model, the equations of state (25)-(28) give the values of the forces and voltage needed to equilibrate with the dielectric in the state $(\lambda_1, \lambda_2, \lambda_3, \tilde{D})$.

In the absence of the applied forces, the stresses in the dielectric vanish. The stresses are zero even when the voltage causes the dielectric to deform. Thus, when the battery applies a voltage to the dielectric, the positive charge on one electrode and the negative charge on the other electrode cause the dielectric to thin down. We simply report what we have observed in this experiment: the voltage causes the dielectric to deform. We do not jump to the conclusion that the voltage causes a compressive stress. In this regard, we view the deformation caused by the voltage in the same way as we view the deformation caused by a change in temperature: both are stress-free deformation, so long as the material is unconstrained^[12].

The work done by the battery, $\Phi \delta Q$, can be written as

$$\Phi \delta Q = (L_3 \tilde{E}) \delta(L_1 L_2 \tilde{D}) = L_1 L_2 L_3 \tilde{E} \delta \tilde{D}. \quad (29)$$

That is, when a dielectric deforms, the nominal electric field and the nominal electric displacement are work-conjugate. By contrast, in terms of the true electric field and the true electric displacement, the work done by the battery is

$$\Phi \delta Q = (l_3 E) \delta(l_1 l_2 D) = l_3 E D \delta(l_1 l_2) + l_1 l_2 l_3 E \delta D. \quad (30)$$

For a deformable dielectric, $\delta(l_1 l_2) \neq 0$, so that the true electric displacement is **not** work-conjugate to the true electric field^[12].

3.2. Vacuum

As an application of the equations of state (25)-(28), consider a block of a vacuum. We think of the vacuum as an elastic dielectric with vanishing rigidity, undergoing a homogenous deformation λ_1 , λ_2 , and λ_3 . Recall an elementary fact that $\epsilon_0 E^2 / 2$ is the electrostatic energy of block divided by the block in the current state. Consequently, the nominal density of free energy is

$$W = \frac{1}{2} \epsilon_0 E^2 \lambda_1 \lambda_2 \lambda_3. \quad (31)$$

Recall that the true electric displacement relates to the true electric field as $D = \epsilon_0 E$, and relates to the nominal electric displacement as $D = \tilde{D} / (\lambda_1 \lambda_2)$. We rewrite (31) in terms of the stretches and the nominal electric displacement:

$$W(\lambda_1, \lambda_2, \lambda_3, \tilde{D}) = \frac{\tilde{D}^2 \lambda_3}{2 \epsilon_0 \lambda_1 \lambda_2}. \quad (32)$$

Inserting (32) into (25)-(28), we obtain that

$$s_1 = -\frac{\tilde{D}^2 \lambda_3}{2 \epsilon_0 \lambda_1^2 \lambda_2}, \quad (33)$$

$$s_2 = -\frac{\tilde{D}^2 \lambda_3}{2\epsilon_0 \lambda_2^2 \lambda_1}, \quad (34)$$

$$s_3 = \frac{\tilde{D}^2}{2\epsilon_0 \lambda_1 \lambda_2}, \quad (35)$$

$$\tilde{E} = \frac{\tilde{D} \lambda_3}{\epsilon_0 \lambda_1 \lambda_2}. \quad (36)$$

Equations (33)-(36) can be expressed in terms of the true quantities as

$$\sigma_1 = -\frac{1}{2} \epsilon_0 E^2, \quad (37)$$

$$\sigma_2 = -\frac{1}{2} \epsilon_0 E^2, \quad (38)$$

$$\sigma_3 = \frac{1}{2} \epsilon_0 E^2, \quad (39)$$

$$D = \epsilon_0 E. \quad (40)$$

Equations (37)-(39) recover the stresses obtained by Maxwell^[40]. They are valid when the electric field is in direction 3.

The Maxwell stress is a tensor. We have already interpreted the component of the Maxwell stress in the direction of the electric field. We now look at the two components of the Maxwell stress transverse to the direction of the electric field. Fig.8 illustrates a classic experiment of a capacitor, which is partly in the air and partly in a dielectric liquid. The applied voltage causes the liquid to rise to a height h . The height results from the balance of the Maxwell stress and the weight of the liquid. The Maxwell stress parallel to the electrodes in the air is $\sigma_a = -\epsilon_a E^2 / 2$, where ϵ_a is the permittivity of the air. The Maxwell stress parallel to the electrodes in the liquid is $\sigma_l = -\epsilon_l E^2 / 2$, where ϵ_l is the permittivity of the liquid. The electric field near the air/liquid interface is distorted, so that the above two formulas are correct only at some distance away from the interface. Because $\epsilon_l > \epsilon_a$, the difference in the Maxwell stresses in the two media will draw the liquid up against gravity. Examining the free-body diagram, and

balancing the electrostatic forces with the weight of the liquid, we obtain that $\rho g h = (\varepsilon_t - \varepsilon_a) E^2 / 2$, where ρg is the weight per unit volume of the liquid.

3.3. Incompressibility

When an elastomer undergoes large deformation, the change in the shape is typically much larger than the change in the volume. Consequently, the elastomer is often taken to be incompressible—that is, the volume of the material remains unchanged during deformation, $l_1 l_2 l_3 = L_1 L_2 L_3$, so that

$$\lambda_1 \lambda_2 \lambda_3 = 1. \quad (41)$$

This assumption of incompressibility places a constraint among the three stretches. We regard λ_1 and λ_2 as independent variables, rewrite (41) as $\lambda_3 = 1/(\lambda_1 \lambda_2)$, and express $\delta \lambda_3$ in terms of $\delta \lambda_1$ and $\delta \lambda_2$:

$$\delta \lambda_3 = -\frac{\delta \lambda_1}{\lambda_1^2 \lambda_2} - \frac{\delta \lambda_2}{\lambda_1 \lambda_2^2}. \quad (42)$$

In terms of the variations of the independent variables, the condition of equilibrium (22) becomes

$$\delta W = \left(s_1 - \frac{s_3}{\lambda_1^2 \lambda_2} \right) \delta \lambda_1 + \left(s_2 - \frac{s_3}{\lambda_2^2 \lambda_1} \right) \delta \lambda_2 + \tilde{E} \delta \tilde{D}. \quad (43)$$

For an incompressible material, this condition of equilibrium holds for any small variations of the three independent variables, λ_1 , λ_2 and \tilde{D} .

For an incompressible elastic dielectric, the density of the free energy is a function of the three independent variables:

$$W = W(\lambda_1, \lambda_2, \tilde{D}). \quad (44)$$

Inserting (44) into (43), we obtain that

$$\left(\frac{\partial W}{\partial \lambda_1} - s_1 + \frac{s_3}{\lambda_1^2 \lambda_2} \right) \delta \lambda_1 + \left(\frac{\partial W}{\partial \lambda_2} - s_2 + \frac{s_3}{\lambda_2^2 \lambda_1} \right) \delta \lambda_2 + \left(\frac{\partial W}{\partial \tilde{D}} - \tilde{E} \right) \delta \tilde{D} = 0. \quad (45)$$

Because $\delta \lambda_1$, $\delta \lambda_2$ and $\delta \tilde{D}$ are independent variations, the condition of equilibrium (45) is equivalent to three equations:

$$s_1 - \frac{s_3}{\lambda_1^2 \lambda_2} = \frac{\partial W(\lambda_1, \lambda_2, \tilde{D})}{\partial \lambda_1}, \quad (46)$$

$$s_2 - \frac{s_3}{\lambda_2^2 \lambda_1} = \frac{\partial W(\lambda_1, \lambda_2, \tilde{D})}{\partial \lambda_2}, \quad (47)$$

$$\tilde{E} = \frac{\partial W(\lambda_1, \lambda_2, \tilde{D})}{\partial \tilde{D}}. \quad (48)$$

The four equations, (41) and (46)-(48), constitute the equations of state for an incompressible dielectric elastomer.

3.4. Ideal Dielectric Elastomers

An elastomer is a three-dimensional network of long and flexible polymers, held together by crosslinks (Fig. 9). Each polymer chain consists of a large number of monomers. Consequently, the crosslinks have negligible effect on the polarization of the monomers: the elastomer can polarize nearly as freely as a polymer melt. The permittivity changes by only a few percent when the area of a membrane of an elastomer is stretched 25 times ^[41]. As an idealization, we may assume that the dielectric behavior of an elastomer is exactly the same as that of a liquid polymer, so that the density of free-energy function takes the form ^[39]

$$W = W_s(\lambda_1, \lambda_2) + \frac{1}{2} \epsilon E^2, \quad (49)$$

where \mathbf{E} is the true electric field, ϵ the permittivity, and $W_s(\lambda_1, \lambda_2)$ the free energy associated with the stretching of the elastomer. The material is also taken to be incompressible, $\lambda_1 \lambda_2 \lambda_3 = 1$.

We call this material model the model of ideal dielectric elastomers.

The true electric displacement relates to the true electric field by $\mathbf{D} = \epsilon \mathbf{E}$, and relates to the nominal electric field as $\mathbf{D} = \tilde{\mathbf{D}}/(\lambda_1 \lambda_2)$. Consequently, in terms the nominal electric displacement, (49) becomes

$$W(\lambda_1, \lambda_2, \tilde{\mathbf{D}}) = W_s(\lambda_1, \lambda_2) + \frac{1}{2\epsilon} \left(\frac{\tilde{\mathbf{D}}}{\lambda_1 \lambda_2} \right)^2. \quad (50)$$

Inspecting (49) and (50), we note that the electromechanical coupling in an ideal dielectric elastomer is purely a geometric effect.

Inserting (50) into (46)-(48) and taking the partial differentiations, we express the results in terms of the true quantities:

$$\sigma_1 - \sigma_3 = \lambda_1 \frac{\partial W_s(\lambda_1, \lambda_2)}{\partial \lambda_1} - \epsilon E^2, \quad (51)$$

$$\sigma_2 - \sigma_3 = \lambda_2 \frac{\partial W_s(\lambda_1, \lambda_2)}{\partial \lambda_2} - \epsilon E^2. \quad (52)$$

$$\mathbf{D} = \epsilon \mathbf{E}. \quad (53)$$

The above expression shows that a through-thickness electric field adds a compressive stress of magnitude ϵE^2 in the two in-plane directions. This set of equations of state has been used almost exclusively in all analyses of dielectric elastomers. The equations are usually justified in terms of the Maxwell stress^[3]. Now we have interpreted these equations using the model of ideal dielectric elastomers. That is, the Maxwell stress is valid when the dielectric behavior of the material is liquid-like, unaffected by deformation.

Observe that, in (51) and (52), the magnitude of the voltage-induced stress is twice the magnitude of the Maxwell stress. This apparent difference is readily understood (Fig.10). Because the elastomer is taken to be incompressible, superposition of a state of hydrostatic stress does not affect the state of deformation. Start from the state of triaxial stresses $(-\epsilon E^2/2, -\epsilon E^2/2, +\epsilon E^2/2)$, as derived by Maxwell, a superposition of a state of hydrostatic

stress $(+\varepsilon E^2/2, +\varepsilon E^2/2, +\varepsilon E^2/2)$ gives a state of uniaxial stress $(0, 0, +\varepsilon E^2)$, and a superposition of a state of hydrostatic stress $(-\varepsilon E^2/2, -\varepsilon E^2/2, -\varepsilon E^2/2)$ gives a state of biaxial stress $(-\varepsilon E^2, -\varepsilon E^2, 0)$. For an incompressible material, the three states of stress illustrated in Fig. 10 cause the same state of deformation.

The free energy due the stretching of the elastomer, $W_s(\lambda_1, \lambda_2)$, may be selected from a large menu of well-tested functions in the theory of rubber elasticity. For example, the neo-Hookean model takes the form

$$W_s = \frac{\mu}{2}(\lambda_1^2 + \lambda_2^2 + \lambda_3^2 - 3), \quad (54)$$

where μ is the small-strain shear modulus.

In an elastomer, each individual polymer chain has a finite contour length. When the elastomer is subject no loads, the polymer chains are coiled, allowing a large number of conformations. Subjected to loads, the polymer chains become less coiled. As the loads increase, the end-to-end distance of each polymer chain approaches the finite contour length, and the elastomer approaches a limiting stretch. On approaching the limiting stretch, the elastomer stiffens steeply. This effect is absent in the neo-Hookean model, but is represented by the Arruda and Boyce model^[43] and the Gent model^[44]. The latter takes the form

$$W_s = -\frac{\mu J_{lim}}{2} \log \left(1 - \frac{\lambda_1^2 + \lambda_2^2 + \lambda_3^2 - 3}{J_{lim}} \right). \quad (55)$$

where μ is the small-stress shear modulus, and J_{lim} is a constant related to the limiting stretch. The stretches are restricted as $0 \leq (\lambda_1^2 + \lambda_2^2 + \lambda_3^2 - 3)/J_{lim} < 1$. When $(\lambda_1^2 + \lambda_2^2 + \lambda_3^2 - 3)/J_{lim} \rightarrow 0$, the Taylor expansion of (55) is (54). That is, the Gent model recovers the neo-Hookean model when deformation is small compared to the limiting stretch. When $(\lambda_1^2 + \lambda_2^2 + \lambda_3^2 - 3)/J_{lim} \rightarrow 1$, the free energy diverges, and the elastomer approaches the limiting stretch.

3.5. Electrostriction

The voltage may cause some dielectrics to become thinner, but other dielectrics to become thicker (Fig. 11). For dielectrics that are nonpolar in the absence of electric field, the voltage-induced deformation has been analyzed by invoking stresses of two origins: electrostriction and the Maxwell stress. The electrostriction results from the effect of deformation on permittivity.

As a simplest model of electrostriction, we expand the free-energy function \mathbf{W} into the Taylor series in powers of \mathbf{E} up to the quadratic term. The expansion is written in the form of (49), but now the permittivity is a function of the stretches:

$$\varepsilon = \varepsilon(\lambda_1, \lambda_2). \quad (56)$$

The same procedure as the above now gives the following equations of state^[45]:

$$\sigma_1 - \sigma_3 = \lambda_1 \frac{\partial W_s(\lambda_1, \lambda_2)}{\partial \lambda_1} - \varepsilon(\lambda_1, \lambda_2) E^2 - \frac{\lambda_1 E^2}{2} \frac{\partial \varepsilon(\lambda_1, \lambda_2)}{\partial \lambda_1}, \quad (57)$$

$$\sigma_2 - \sigma_3 = \lambda_2 \frac{\partial W_s(\lambda_1, \lambda_2)}{\partial \lambda_2} - \varepsilon(\lambda_1, \lambda_2) E^2 - \frac{\lambda_2 E^2}{2} \frac{\partial \varepsilon(\lambda_1, \lambda_2)}{\partial \lambda_2}, \quad (58)$$

$$\mathbf{D} = \varepsilon(\lambda_1, \lambda_2) \mathbf{E}. \quad (59)$$

The variation of the permittivity with stretches has been observed experimentally^[46]. Further measurements are needed to ascertain the practical significance of electrostriction in dielectric elastomers.

IV. NONEQUILIBRIUM THERMODYNAMICS OF DIELECTRIC ELASTOMERS

An elastomer responds to forces and voltage by time-dependent, dissipative processes^[47-49]. Viscoelastic relaxation may result from slippage between long polymers and rotation of joints between monomers. Dielectric relaxation may result from distortion of electron clouds and rotation of polar groups. Conductive relaxation may result from migration of electrons and ions through the elastomer. This section describes an approach to construct models of

dissipative dielectric elastomers, guided by nonequilibrium thermodynamics^[50].

Thermodynamics requires that the increase in the free energy should not exceed the total work done, namely,

$$\delta F \leq P_1 \delta \mathbf{L}_1 + P_2 \delta \mathbf{L}_2 + P_3 \delta \mathbf{L}_3 + \Phi \delta Q. \quad (60)$$

For the inequality to be meaningful, the small changes are time-directed: $\delta \mathbf{f}$ means the change of the quantity \mathbf{f} from one time to a slightly later time.

Divide both sides of (60) by the volume of the membrane, $\mathbf{L}_1 \mathbf{L}_2 \mathbf{L}_3$, and the thermodynamic inequality becomes

$$\delta W \leq s_1 \delta \lambda_1 + s_2 \delta \lambda_2 + s_3 \delta \lambda_3 + \tilde{E} \delta \tilde{D}. \quad (61)$$

As a model of the dielectric elastomer, the free-energy density is prescribed as a function:

$$W = W(\lambda_1, \lambda_2, \lambda_3, \tilde{D}, \xi_1, \xi_2, \dots). \quad (62)$$

We characterize the state of a dielectric by $\lambda_1, \lambda_2, \lambda_3$ and \tilde{D} , along with additional parameters (ξ_1, ξ_2, \dots) . Inspecting (61), we note that $\lambda_1, \lambda_2, \lambda_3$ and \tilde{D} are the kinematic parameters through which the external loads do work. By contrast, the additional parameters (ξ_1, ξ_2, \dots) are not associated with the external loads in this way. These additional parameters describe the degrees of freedom associated with dissipative processes, and are known as internal variables.

Inserting (62) into (61), we rewrite the thermodynamic inequality as

$$\left(\frac{\partial W}{\partial \lambda_1} - s_1 \right) \delta \lambda_1 + \left(\frac{\partial W}{\partial \lambda_2} - s_2 \right) \delta \lambda_2 + \left(\frac{\partial W}{\partial \lambda_3} - s_3 \right) \delta \lambda_3 + \left(\frac{\partial W}{\partial \tilde{D}} - \tilde{E} \right) \delta \tilde{D} + \sum_i \frac{\partial W}{\partial \xi_i} \delta \xi_i \leq 0. \quad (63)$$

As time goes forward, this thermodynamic inequality holds for any change in the independent variables $(\lambda_1, \lambda_2, \lambda_3, \tilde{D}, \xi_1, \xi_2, \dots)$. We next specify a model consistent with this inequality.

We assume that the system is in mechanical and electrostatic equilibrium, so that in (63) the factors in front of $\delta \lambda_1, \delta \lambda_2$ and $\delta \tilde{D}$ vanish:

$$s_1 = \frac{\partial W(\lambda_1, \lambda_2, \lambda_3, \tilde{D}, \xi_1, \xi_2, \dots)}{\partial \lambda_1}, \quad (64)$$

$$s_2 = \frac{\partial W(\lambda_1, \lambda_2, \lambda_3, \tilde{D}, \xi_1, \xi_2, \dots)}{\partial \lambda_2}, \quad (65)$$

$$s_3 = \frac{\partial W(\lambda_1, \lambda_2, \lambda_3, \tilde{D}, \xi_1, \xi_2, \dots)}{\partial \lambda_3}, \quad (66)$$

$$\tilde{E} = \frac{\partial W(\lambda_1, \lambda_2, \lambda_3, \tilde{D}, \xi_1, \xi_2, \dots)}{\partial \tilde{D}}. \quad (67)$$

Equations (64)-(67) constitute the thermodynamic equations of state of the dielectric elastomer.

Once the elastomer is assumed to be in mechanical and electrostatic equilibrium, the inequality (63) becomes

$$\sum_i \frac{\partial W(\lambda_1, \lambda_2, \lambda_3, \tilde{D}, \xi_1, \xi_2, \dots)}{\partial \xi_i} \delta \xi_i \leq 0. \quad (68)$$

This thermodynamic inequality may be satisfied by prescribing a suitable relation between $(\delta \xi_1, \delta \xi_2, \dots)$ and $(\partial W / \partial \xi_1, \partial W / \partial \xi_2, \dots)$. For example, one may adopt a kinetic model of the type

$$\frac{d \xi_i}{dt} = - \sum_j M_{ij} \frac{\partial W(\lambda_1, \lambda_2, \lambda_3, \tilde{D}, \xi_1, \xi_2, \dots)}{\partial \xi_j}. \quad (69)$$

Here \mathbf{M}_{ij} is a positive-definite matrix, which may depend on the independent variables $(\lambda_1, \lambda_2, \lambda_3, \tilde{D}, \xi_1, \xi_2, \dots)$.

To represent a dissipative dielectric elastomer using the above approach, we need to specify a set of internal variables (ξ_1, ξ_2, \dots) , and then specify the functions $W(\lambda_1, \lambda_2, \lambda_3, \tilde{D}, \xi_1, \xi_2, \dots)$ and $\mathbf{M}_{ij}(\lambda_1, \lambda_2, \lambda_3, \tilde{D}, \xi_1, \xi_2, \dots)$. There is considerable flexibility in choosing kinetic models to fulfill the thermodynamic inequality (68).

Viscoelastic relaxation is commonly pictured with an array of springs and dashpots, known as the rheological models; see a recent example^[51]. Similarly, dielectric relaxation is

commonly pictured with models consisting of resistors and capacitors. By contrast, electrical conduction involves the transport of charged species over a long distance. Coupled large deformation and transport of charged species are significant in polyelectrolytes^[21], and will not be discussed here.

V. ELECTROMECHANICAL INSTABILITY

While all dielectrics deform under voltage, the amount of deformation differs markedly among different materials. Under voltage, piezoelectric ceramics attain strains of typically less than 1%. Glassy and semi-crystalline polymers can attain less than 10%^[52]. Strains about 30% were observed in some elastomers^[53]. In the last decade, strains over 100% have been achieved in several ways, by pre-stretching an elastomer^[3], by using an elastomer of interpenetrating networks^[54,55], by swelling an elastomer with a solvent^[56], and by spraying charge on an electrode-free elastomer^[57].

These experimental advances have prompted a theoretical question: What is the fundamental limit of deformation that can be induced by voltage? One can easily increase the length of a rubber band several times by using a mechanical force. Why is it difficult to do so by using a voltage? The difficulty has to do with two modes of failure associated with apply a voltage: electrical breakdown and electromechanical instability. For a stiff dielectric such as a ceramic or a glassy polymer, voltage-induced deformation is limited by electrical breakdown, when the voltage mobilizes charged species in the dielectric to produce a path of electrical conduction.

For a compliant dielectric such as an elastomer, the voltage-induced deformation is often limited by electromechanical instability. It was Stark and Garton^[58] who first reported that the breakdown fields of polymers reduced when the polymers became soft at elevated temperatures. The phenomenon is understood as follows. The electric voltage is applied between the electrodes on the top and the bottom surfaces of a thin layer of a polymer. As the

electric field increases, the polymer thins down, so that the same voltage will induce an even higher electric field. This positive feedback results in a mode of instability, known as electromechanical instability or pull-in instability, which causes the polymer to reduce the thickness drastically, often leading to electrical breakdown. Electromechanical instability has been recognized as a failure mode of the insulators for power transmission cables.

Electromechanical instability is sensitive to the stress-stretch behavior of the elastomer^[39]. Fig. 12a sketches a dielectric membrane pulled by biaxial stresses σ . The length of the membrane in any direction in the plane is stretched by a ratio λ . As will become clear, to attain a large voltage-induced stretch, the dielectric should have a stress-stretch curve $\sigma(\lambda)$ of the following desirable features^[59]: (a) The dielectric is compliant at small stretches, and (b) the dielectric stiffens steeply at modest stretches. That is, the limiting stretch, λ_{lim} , should not be excessive. Also sketched are several designs of materials that exhibit the stress-stretch curve of the desirable form. Many biological tissues, such as skins and vascular walls, deform readily, but avert excessive deformation. Fig. 12b sketches a design of such a tissue, consisting of stiffer fibers in a compliant matrix. At small stretches, the fibers are loose, and the tissue is compliant. At large stretches, the fibers are taut, and the tissue stiffens steeply. As another example, Fig. 12c sketches a network of polymers with folded domains. The domains unfold when the network is pulled, giving rise to substantial deformation. After all the domains unfold, the network stiffens steeply.

Consider a synthetic elastomer, i.e., a network of polymer chains. When the individual chains are short, the initial modulus of the elastomer is large and the limiting stretch λ_{lim} is small. When the individual chains are long, the initial modulus of the elastomer is small and the limiting stretch λ_{lim} is large. Consequently, it is difficult to achieve the stress-stretch curve of the desirable form by adjusting the density of crosslinks alone. The stress-stretch curve, however, can be shaped into the desirable form in several ways. For example, the widely used

dielectric elastomer, VHB, is a network of polymers with side chains (Fig. 12d). The side chains fill the space around the networked chains. The motion of the networked chains is lubricated, lowering the glass transition temperature. Also the density of the networked chains is reduced, lowering the stiffness of the elastomer when the stretch is small. While the side chains do not change the contour length of the networked chains, the side chains pull the networked chains towards their full contour length even when the elastomer is not loaded. Once loaded, the elastomer may stiffen sharply, averting electromechanical instability. Similar behavior is expected for a network swollen with a solvent (Fig. 12e). The stress-stretch curve can also be shaped into the desirable form by prestretch^[3], or by using interpenetrating networks^[54,55].

As illustrated in Fig. 13a, when a membrane of an elastomer, thickness H in the undeformed state, is subject to a voltage Φ , the membrane is stretched by λ in both directions in the plane, the thickness of the membrane reduces to $H\lambda^{-2}$, and the electric field in the membrane is $E = \lambda^2 \Phi / H$. The membrane is taken to be incompressible. The actuation can be described by the Maxwell stress. A combination of the above considerations relates the voltage to the stretch:

$$\Phi = H\lambda^{-2} \sqrt{\sigma(\lambda) / \epsilon}. \quad (70)$$

This voltage-stretch relation is sketched in Fig. 13a. Even though the stress-stretch curve $\sigma(\lambda)$ is monotonic, the voltage-stretch curve $\Phi(\lambda)$ is usually not^[39]. At a small stretch ($\lambda \sim 1$), the rising $\sigma(\lambda)$ dominates, and the voltage increases with the stretch. At an intermediate stretch, the factor λ^{-2} due to thinning of the membrane becomes important, and the voltage falls as the stretch increases. As the elastomer approaches the limiting stretch λ_{lim} , the steep rise of $\sigma(\lambda)$ prevails, and the voltage rises again. The shape of the voltage-stretch curve $\Phi(\lambda)$ indicates a snap-through electromechanical instability^[39]. The instability can cause some regions of the elastomer to thin down more than others.

The local maximum voltage represents a critical condition, which can be estimated as follows. Under the equal-biaxial stresses, Hooke's law takes the form $\sigma(\lambda) = 6\mu(\lambda - 1)$, where μ is the shear modulus. Inserting this expression into (70), and maximizing the function $\Phi(\lambda)$, we find local maximum voltage $\Phi_c \approx 0.80H\sqrt{\mu/\epsilon}$ and the critical $\lambda_c = 4/3 = 1.33$. The critical values vary somewhat with the stress-stretch relation. For example, for the neo-Hookean model, $\sigma(\lambda) = \mu(\lambda^2 - \lambda^{-4})$, the maximum voltage is $\Phi_c \approx 0.69H\sqrt{\mu/\epsilon}$ and the critical stretch is $\lambda_c = 2^{1/3} \approx 1.26$. This electromechanical instability has been analyzed systematically by using the Hessian [60-64].

Before a voltage is applied, an elastomer may be prestretched to λ by a mechanical force, and then fixed by rigid electrodes. Subsequently, when the voltage is applied, the elastomer will not deform further. The measured voltage at failure is taken to be the electrical breakdown voltage. Experiments indicate that the breakdown voltage is a monotonically decreasing function of the prestretch, $\Phi_B(\lambda)$ [30,41].

According to where the curves $\Phi(\lambda)$ and $\Phi_B(\lambda)$ intersect, we distinguish three types of dielectric elastomers[59]. A type I dielectric suffers electrical breakdown prior to electromechanical instability, and is capable of small deformation of actuation, Fig. 13b. A type II dielectric reaches the peak of the $\Phi(\lambda)$ curve, and thins down excessively, leading to electrical breakdown, Fig. 13c. The dielectric is recorded to fail at the peak of $\Phi(\lambda)$, which can be much below the breakdown voltage Φ_B . The deformation of actuation is limited by the stretch at which the voltage reaches the peak. A type III dielectric eliminates or survives electromechanical instability, reaches a stable state before the electrical breakdown, and attains a large deformation of actuation, Fig. 13d.

A new experimental manifestation of the electromechanical instability has been reported recently[30]. Under certain conditions, an electric voltage can deform a layer of a

dielectric elastomer into a mixture of two regions, one being flat and the other wrinkled (Fig. 14). In the experiment, the electrodes on the top and the bottom surfaces of the dielectric layer were made of conducting grease, which applied a uniform electric potential to the elastomer without constraining its deformation. This observation has been interpreted as the coexistence of two states^[39].

VI. INHOMOGENEOUS FIELDS

Studies of inhomogeneous fields of coupled large deformation and electric potential date back to classic works of Toupin^[66], Eringen^[67] and Tiersten^[68]. These works have been reexamined recently for applications to dielectric elastomers^[9-13]. Here we summarize basic ideas, following the presentation of Ref. [12].

6.1. Condition of Thermodynamic Equilibrium

A body of an elastic dielectric is represented by a field of material particles. Each material particle is named after the coordinate \mathbf{X} of its place when the body is in a reference state. In the current state, at time t , the particle \mathbf{X} moves to a place with coordinate \mathbf{x} . The function

$$\mathbf{x} = \mathbf{x}(\mathbf{X}, t) \quad (71)$$

describes the history of the deformation of the body. Define the deformation gradient \mathbf{F} as

$$F_{ik} = \frac{\partial x_i(\mathbf{X}, t)}{\partial X_k}. \quad (72)$$

The deformation gradient generalizes the notion of the stretches.

In the current state at time t , the electric potential at particle \mathbf{X} is denoted as

$$\Phi = \Phi(\mathbf{X}, t). \quad (73)$$

The gradient of the electric potential defines the nominal electric field $\tilde{\mathbf{E}}$, namely,

$$\tilde{E}_K = -\frac{\partial \Phi(\mathbf{X}, t)}{\partial X_K}. \quad (74)$$

The negative sign in (74) follows the convention that the electric field vector points in the direction from a particle of a high voltage to a particle of a low voltage.

Motivated by (22), we write the variation of the nominal Helmholtz free energy, δW , in the form:

$$\delta W = s_{iK} \delta F_{iK} + \tilde{E}_K \delta \tilde{D}_K, \quad (75)$$

where δF_{iK} is a small change in the deformation gradient, and $\delta \tilde{D}_K$ is a small change in the nominal electric field. Equation (75) defines the nominal stress \mathbf{s} as a tensor work-conjugate to the deformation gradient \mathbf{F} , and the nominal electric displacement $\tilde{\mathbf{D}}$ as a vector work-conjugate to the nominal electric field $\tilde{\mathbf{E}}$.

Inspecting (72) and (74), we wish to use the deformation gradient and the nominal electric field as the independent variables. Introducing a new quantity \hat{W} by

$$\hat{W} = W - \tilde{E}_K \tilde{D}_K. \quad (76)$$

The quantity \hat{W} may be called the electrical Gibbs free energy. A combination of (75) and (76) gives

$$\delta \hat{W} = s_{iK} \delta F_{iK} - \tilde{D}_K \delta \tilde{E}_K. \quad (77)$$

We may call the quantity $\tilde{D}_K \delta \tilde{E}_K$ the complementary electrical work.

A material model is prescribed by a function $\hat{W} = \hat{W}(\mathbf{F}, \tilde{\mathbf{E}})$. When the body undergoes a rigid body motion, the free energy is invariant. Consequently, the function depends on the deformation gradient through the Green deformation tensor, $\mathbf{C}_{KL} = \mathbf{F}_{iK} \mathbf{F}_{iL}$. Associated with small changes δF_{iK} and $\delta \tilde{E}_K$, the electrical Gibbs free energy changes by

$$\delta \hat{W} = \frac{\partial \hat{W}(\mathbf{F}, \tilde{\mathbf{E}})}{\partial F_{iK}} \delta F_{iK} + \frac{\partial \hat{W}(\mathbf{F}, \tilde{\mathbf{E}})}{\partial \tilde{E}_K} \delta \tilde{E}_K. \quad (78)$$

On each material element of volume $dV(\mathbf{X})$, we prescribe mass $\rho(\mathbf{X})dV$, force $\mathbf{B}(\mathbf{X},t)dV$ and charge $q(\mathbf{X},t)dV$. The effect of inertia may be represented by adding to the force the inertial force, so that the net force on the element of volume is $(\mathbf{B}_i - \rho \partial^2 \mathbf{x}_i / \partial t^2) \delta \mathbf{x}_i dV$. On each material element of interface $dA(\mathbf{X})$, we prescribe force $\mathbf{T}(\mathbf{X},t)dA$ and charge $\omega(\mathbf{X},t)dA$.

Let $\delta \mathbf{x}_i = \Delta_i(\mathbf{X})$ be a field of virtual displacement of the body—that is, every material particle \mathbf{X} moves independently. The virtual displacement $\Delta_i(\mathbf{X})$ is unrelated to actual displacement $\mathbf{x}_i(\mathbf{X},t)$. Associated with the field of virtual displacement, the forces do virtual work $\int (\mathbf{B}_i - \rho \partial^2 \mathbf{x}_i / \partial t^2) \delta \mathbf{x}_i dV + \int T_i \delta \mathbf{x}_i dA$. Similarly, let $\delta \Phi = \eta(\mathbf{X})$ be a field of virtual electric potential of the body. Associated with the field of electric potential, the charges do virtual complementary work $\int q \delta \Phi dV + \int \omega \delta \Phi dA$. The virtual deformation gradient is $\delta F_{iK} = \partial \Delta_i(\mathbf{X}) / \partial X_K$, the virtual nominal electric field is $\delta \tilde{\mathbf{E}}_K = -\partial \eta(\mathbf{X}) / \partial X_K$, and the virtual change in the electrical Gibbs free energy is $\int \delta \hat{W} dV$, where $\delta \hat{W}$ is given by (78). When the body is in thermodynamic equilibrium, the change in the electrical Gibbs free energy equals the mechanical work minus the complementary electrical work:

$$\int \delta \hat{W} dV = \int \left(B_i - \rho \frac{\partial^2 \mathbf{x}_i}{\partial t^2} \right) \delta \mathbf{x}_i dV + \int T_i \delta \mathbf{x}_i dA - \int q \delta \Phi dV - \int \omega \delta \Phi dA. \quad (79)$$

This condition of thermodynamic equilibrium has the similar physical content as (1) and (21), and holds for arbitrary and independent variations $\delta \mathbf{x}$ and $\delta \Phi$.

Once the loads and the electrical Gibbs free-energy function $\hat{W}(\mathbf{F}, \tilde{\mathbf{E}})$ are prescribed, the variational statement (79), along with the definitions (72) and (74), is the basis for the finite element method, determining the field of deformation $\mathbf{x}(\mathbf{X},t)$ and the field of electric potential $\Phi(\mathbf{X},t)$ simultaneously. Several implementations of the finite element method have been

reported^[65,69-71], but few practical examples are available, especially transducers approach electromechanical instability. Significant effort is needed to develop the finite element method, and to apply the method to analyze phenomena and devices.

6.2. Differential Equations

The variational statement of thermodynamic equilibrium also leads to partial differential equations. These equations are listed in this subsection.

A comparison of (77) and (78) gives that

$$s_{iK} = \frac{\partial \hat{W}(\mathbf{F}, \tilde{\mathbf{E}})}{\partial F_{iK}}, \quad (80)$$

$$\tilde{D}_K = -\frac{\partial \hat{W}(\mathbf{F}, \tilde{\mathbf{E}})}{\partial \tilde{E}_K}. \quad (81)$$

Once the electrical free-energy function $\hat{W}(\mathbf{F}, \tilde{\mathbf{E}})$ is prescribed, (80) and (81) constitute the equations of states.

Inserting (72), (74) and (77) into the condition of thermodynamic equilibrium (79), and recalling that the condition holds for arbitrary and independent variations in $\delta \mathbf{x}$ and $\delta \Phi$, we obtain that

$$\frac{\partial s_{iK}(\mathbf{X}, t)}{\partial X_K} + B_i(\mathbf{X}, t) = \rho(\mathbf{X}) \frac{\partial^2 x_i(\mathbf{X}, t)}{\partial t^2} \quad (82)$$

in the volume

$$(s_{iK}^- - s_{iK}^+) N_K = T_i \quad (83)$$

on an interface,

$$\frac{\partial \tilde{D}_K(\mathbf{X}, t)}{\partial X_K} = q(\mathbf{X}, t) \quad (84)$$

in the volume, and

$$(\tilde{D}_K^+ - \tilde{D}_K^-) N_K = \omega(\mathbf{X}, t) \quad (85)$$

on the interfaces. Equations (82) and (83) reproduce the equations for momentum balance, and (84) and (85) reproduce Gauss's law of electrostatics.

Equations (71)-(74) and (80)-(85) are governing equations to determine the field of deformation $\mathbf{x}(\mathbf{X}, t)$ and the field of electric potential $\Phi(\mathbf{X}, t)$ simultaneously, once the loads and the free-energy function $\hat{W}(\mathbf{F}, \tilde{\mathbf{E}})$ are prescribed. These partial differential equations have been used to solve boundary-value problems involving coupled large deformation electric potential^[72-76]. Observe that the equations of mechanics, (71), (72), (82) and (83), decouple from those of electrostatics, (73), (74), (84) and (85). The only coupling between mechanics and electrostatics arises from the material model, (80) and (81).

6.3. True Quantities

The true stress σ_{ij} relates to the nominal stress by

$$\sigma_{ij} = \frac{F_{jK}}{\det \mathbf{F}} s_{iK} . \quad (86)$$

The true electric displacement D_i relates to the nominal electric displacement as

$$D_i = \frac{F_{iK}}{\det \mathbf{F}} \tilde{D}_K . \quad (87)$$

The true electric field E_i relates to the nominal electric field as

$$E_i = H_{iK} \tilde{E}_K , \quad (88)$$

where H_{iK} is the inverse of the deformation gradient, namely, $H_{iK} F_{iL} = \delta_{KL}$ and $H_{iK} F_{jK} = \delta_{ij}$.

The true quantities are functions of \mathbf{x} and t , and satisfy the familiar partial differential equations in mechanics and electrostatics.

6.4. Ideal Dielectric Elastomers

Toupin^[66] noted that, for an isotropic elastic dielectric, the free-energy density is a

function of six invariants of the deformation gradient tensor and the electric field vector. Function of this complexity is unavailable for any real material. Several further considerations may reduce the complexity of the free-energy function somewhat, but are still far from being useful in practice^[12].

We next describe ideal dielectric elastomers—a material model nearly exclusively used in the literature. As discussed before in connection with Fig. 9, for an ideal dielectric elastomer, the dielectric behavior is the same as that of a liquid—that is, the dielectric behavior is unaffected by deformation^[39]. As a simplest model of a dielectric liquid, assume that the true electric displacement \mathbf{D}_m is linear in the true electric field \mathbf{E}_m :

$$\mathbf{D}_m = \varepsilon \mathbf{E}_m \quad (89)$$

The permittivity ε is taken to be independent of deformation.

Using (87) and (88), we express (89) in terms of the nominal fields:

$$\tilde{\mathbf{D}}_N = \varepsilon \tilde{\mathbf{E}}_L \mathbf{H}_{mN} \mathbf{H}_{mL} \det \mathbf{F}. \quad (90)$$

Inserting (90) into (81) and integrating, we obtain the nominal density of the electrical Gibbs free energy:

$$\hat{W}(\mathbf{F}, \tilde{\mathbf{E}}) = W_s(\mathbf{F}) - \frac{\varepsilon}{2} \tilde{\mathbf{E}}_N \tilde{\mathbf{E}}_L \mathbf{H}_{mN} \mathbf{H}_{mL} \det \mathbf{F}. \quad (91)$$

Here $W_s(\mathbf{F})$ is the free energy associated with the strength of the elastomer, which may be selected from a large menu in the theory of elasticity. While the elastomer is nearly incompressible, in the finite element method, it is convenient to allow the material to be compressible with a large bulk modulus.

Insert (91) into (80), and recall mathematical identities $\partial \mathbf{H}_{mN} / \partial \mathbf{F}_{iK} = -\mathbf{H}_{mK} \mathbf{H}_{iN}$ and $\partial \det \mathbf{F} / \partial \mathbf{F}_{iK} = \mathbf{H}_{iK} \det \mathbf{F}$. We obtain that

$$\mathbf{s}_{iK} = \frac{\partial W_s(\mathbf{F})}{\partial \mathbf{F}_{iK}} + \varepsilon \tilde{\mathbf{E}}_N \tilde{\mathbf{E}}_L \left(\mathbf{H}_{iN} \mathbf{H}_{mK} \mathbf{H}_{mL} - \frac{1}{2} \mathbf{H}_{mN} \mathbf{H}_{mL} \mathbf{H}_{iK} \right) \det \mathbf{F}. \quad (92)$$

This equation of state expresses the nominal stress as a function of the deformation gradient and the nominal electric field.

A combination of (86) and (92) gives

$$\sigma_{ij} = \frac{F_{jK}}{\det \mathbf{F}} \frac{\partial W_s(\mathbf{F})}{\partial F_{iK}} + \varepsilon \left(E_i E_j - \frac{1}{2} E_m E_m \delta_{ij} \right). \quad (93)$$

This equation expresses the true stress as a function of the deformation gradient and the true electric field. The contribution due to the deformation gradient results of the stretching of the elastomer, and is the same as that in the theory of elasticity. The contribution due to the electric field is identical to that derived by Maxwell^[40]. When $\sigma_{ij} = 0$, (93) balances elasticity and electrostatics, and determines the voltage-induced deformation. As commented before, the Maxwell stress correctly accounts for the voltage-induced deformation only when the dielectric behavior is liquid-like, an idealization works well with elastomers, but not for any other solid dielectrics.

Equations (89) and (93) constitute the equations of state, for an ideal dielectric elastomer, in terms of the true quantities. The equations of state exhibit one-way coupling: the deformation does not affect the dielectric behavior, but the electric field contributes to the stress-stretch relation. As noted before, the partial differential equations of mechanics decouples from those of electrostatics. One may solve electrostatic boundary-value problems in terms of the true fields, and then add the Maxwell stress in solving the elastic field. Of course, the deformation will change the shape of the boundaries of the body. This change must be included in solving the electrostatic problems. The one-way coupling may not bring any advantage after all.

The model of ideal dielectric elastomers can be generalized to account for nonlinear dielectric behavior, by replacing (89) with a nonlinear relation between the electric field and electric displacement^[12]. Nonlinear dielectric behavior may be significant at high electric fields. Furthermore, the model of ideal dielectric elastomers can be modified to include dissipative

processes, such as viscoelasticity, dielectric relaxation, and electrical conduction^[21,50].

VII. CONCLUDING REMARKS

A large number of examples in biology demonstrate that deformation of soft materials connect diverse stimuli to many functions essential to the life. An exciting field of engineering is emerging that uses soft active materials to create soft machines. To participate in advancing the field of soft active materials and soft machines effectively, mechanicians must retool our laboratories and our software, as well as adapt our theories. While theories are being developed for diverse soft active materials, this review focuses on one class of soft active materials: dielectric elastomers. This focus allows us to review the theory in some depth, within the framework of nonlinear continuum mechanics and nonequilibrium thermodynamics, while motivating the theory by empirical observations, molecular pictures and applications. It is hoped that the theory will be used to develop software, study intriguing phenomena of electromechanical coupling, and aid the creation of soft active materials and soft machines.

References

1. Mathger, L.M., Denton, E.J., Marshall, N.J. and Hanlon, R.T., Mechanisms and behavioral functions of structural coloration in cephalopods, *J. R. Soc. Interface*, 2008, 6: S149-S163.
2. Zwieniecki, M.A., Melcher, P.J. and Holbrook, N.M., Hydrogel control of xylem hydraulic resistance in plants, *Science*, 2001, 291: 1059-1062.
3. Pelrine, R., Kornbluh, R., Pei, Q.B. and Joseph, J., High-speed electrically actuated elastomers with strain greater than 100%, *Science*, 2000, 287: 836-839.
4. Tanaka, T., Gels, *Sci. Am.*, 1981, Jan. 244: 124-138.
5. Beebe, D.J., Moore, J.S., Bauer, J.M., Yu, Q., Liu, R.H., Devadoss, C. and Jo, B.H., Functional hydrogel structures for autonomous flow control inside microfluidic channels, *Nature*, 2000, 404: 588-590.
6. Calvert, P., Hydrogels for soft machines, *Adv. Mater.*, 2009, 21: 743-756.
7. Liu, F. and Urban, M.W., Recent advances and challenges in designing stimuli-responsive polymers, *Prog. Polymer Sci.*, 2010, 35: 3-23.
8. Cai, S.Q., Lou, Y.C., Ganguly, P., Robisson, A., Suo, Z.G., Force generated by a swelling elastomer subject to constraint. *J. Appl. Phys.*, 2010, 107: 103535.
9. Goulbourne, N.C., Mockensturm, E.M., Frecker, M., A nonlinear model for dielectric elastomer membranes, *J. Appl. Mech.*, 2005, 72: 899-906.
10. Dorfmann, A. and Ogden, R.W., Nonlinear electroelasticity, *Acta Mechanica*, 2005, 174: 167-183.
11. McMeeking, R. M. and Landis, C.M., Electrostatic forces and stored energy for deformable dielectric materials. *J. Appl. Mech.*, 2005, 72: 581-590.
12. Suo, Z.G., Zhao, X.H. and Greene, W.H., A nonlinear field theory of deformable dielectrics, *J. Mech. Phys. Solids*, 2008, 56: 467-286.
13. Trimarco, C., On the Lagrangian electrostatics of elastic solids, *Acta Mech.*, 2009, 204: 193-201.
14. Sekimoto, K., Thermodynamics and hydrodynamics of chemical gels, *J. Phys. II*, 1991, 1, 19-36.
15. Dolbow, J., Fried, E., Jia, H.D., Chemically induced swelling of hydrogels. *J. Mech. Phys. Solids*, 2004, 52: 51-84.
16. Baek, S. and Srinivasa, A.R., Diffusion of a fluid through an elastic solid undergoing large deformation, *Int. J. Non-linear Mech.*, 2004, 39: 201-218.
17. Hong, W., Zhao, X.H., Zhou, J.X. and Suo, Z.G., A theory of coupled diffusion and large deformation in polymeric gels. *J. Mech. Phys. Solids*, 2008, 56: 1779-1793.
18. Doi, M., Gel dynamics, *J. Phys. Soc. Japan*, 2009, 78: 052001.
19. Chester, S.A. and Anand, L., A coupled theory of fluid permeation and large deformations for elastomeric materials, *J. Mech. Phys. Solids*, 2010, 58: 1879-1906.
20. Nemat-Nasser, S. and Li, J.Y., Electromechanical response of ionic polymer-metal composites, *J. Appl. Phys.*, 2000, 87: 3321-3331.
21. Hong, W., Zhao, X.H., Suo, Z.G., Large deformation and electrochemistry of polyelectrolyte gels, *J. Mech. Phys. Solids*, 2010, 58: 558-577.
22. Baek, S. and Srinivasa, A.R., Modeling of the pH-sensitive behavior of an ionic gel in the presence of diffusion. *Int. J. Non-linear Mech.*, 2004, 39: 1301-1318.
23. Li, H., Luo, R., Birgersson, E., Lam, K.Y., Modeling of multiphase smart hydrogels responding to pH and electric voltage coupled stimuli, *J. Appl. Phys.*, 2007, 101: 114905.
24. Marcombe, R., Cai, S.Q., Hong, W., Zhao, X.H., Lapusta, Y., and Suo, Z.G., A theory of constrained swelling of a pH-sensitive hydrogel, *Soft Matter*, 2010, 6: 784-793.
25. Cai, S.Q. and Suo, Z.G., Mechanics and chemical thermodynamics of a temperature-sensitive hydrogel. Manuscript in preparation.

26. Shankar, R., Ghosh, T.K. and Spontak, R.J., Dielectric elastomers as next-generation polymeric actuators, *Soft Matter*, 2007, 3: 1116-1129.
27. Carpi, F., Electromechanically active polymers, Editorial introducing a special issue dedicated to dielectric elastomers, *Polymer International*, 2010, 59:277-278.
28. Brochu, P. and Pei, Q. B., Advances in dielectric elastomers for actuators and artificial muscles, *Macromolecular Rapid Communications*, 2010, 31: 10-36.
29. Gibbs, J.W., Graphical methods in the thermodynamics of fluids, *Transactions of the Connecticut Academy*, 1973, 2:309-342. (Available online at Google Books)
30. Plante, J.S. and Dubowsky, S., Large-scale failure modes of dielectric elastomer actuators, *Int. J. Solids Structures*, 2006, 43: 7727-7751.
31. Wissler, M. and Mazza, E., Mechanical behavior of acrylic elastomer used in dielectric elastomer actuators, *Sensors Actuators A*, 2007, 134: 494-504.
32. Kollosche, M. and Kofod, G., Electrical failure in blends of chemically identical, soft thermoplastic elastomers with different elastic stiffness, *Appl. Phys. Lett.*, 2010, 96: 071904.
33. Lochmatter, P., Kovacs, G., and Michel, S., Characterization of dielectric elastomer actuators based on a hyperelastic film model, *Sensors and Actuators A*, 2007, 135: 748-757.
34. Moscardo, M., Zhao, X.H., Suo, Z.G. and Lapusta, Y., On designing dielectric elastomer actuators, *J. Appl. Phys.*, 2008, 104: 093503.
35. Koh, S.J.A., Zhao, X.H. and Suo, Z.G., Maximal energy that can be converted by a dielectric elastomer generator. *Appl. Phys. Lett.*, 2009, 94: 262902.
36. Koh, S.J.A., Keplinger, C., Li, T.F., Bauer, S. and Suo, Z.G., Dielectric elastomer generators: How much energy can be converted? *Transactions on Mechatronics*, in press.
37. Diaz-Calleja, R., Llovera-Segovia, P., Energy diagrams and stability restrictions for electroelastic generators, *J. Polymer Sci. B*, 2010, 48: 2023-2028.
38. Gibbs, J.W., A method of geometrical representation of the thermodynamic properties of substances by means of surfaces, *Transactions of the Connecticut Academy*, 1973, 2:382-404. (Available online at Google Books)
39. Zhao, X.H., Hong, W. and Suo, Z.G., Electromechanical coexistent states and hysteresis in dielectric elastomers, *Phys. Rev. B*, 2007, 76: 134113.
40. Maxwell, J.C., A Treatise on Electricity and Magnetism, Volume 1, Chapter V, Mechanical action between two electrical systems, Oxford University Press, 1873. (Available online at Google Books)
41. Kofod, G., Sommer-Larsen, P., Kornbluh, R. and Pelrine, R., Actuation response of polyacrylate dielectric elastomers, *J. Intell. Mater. Syst. Struct.*, 2003, 14: 787-793.
42. Treloar, L.R.G., The Physics of Rubber Elasticity, Oxford University Press, 1975.
43. Arruda, E. M. and Boyce, M. C. *J. Mech. Phys. Solids* **41**, 389-412 (1993).
44. Gent, A. N., *Rubber Chem. Technol* **69**, 59-61 (1996).
45. Zhao X. and Suo, Z.G., Electrostriction in elastic dielectrics undergoing large deformation, *J. Appl. Phys.*, 2008, 104: 123530.
46. Wissler, M. and Mazza, E., Electromechanical coupling in dielectric elastomer actuators, *Sensors and Actuators A*, 2007, 138: 384-393.
47. Lochmatter, P., Kovacs, G., Wissler, M., Characterization of dielectric elastomers based on a visco-hyperelastic film model, *Smart Mater. Structures*, 2007, 135: 748-757.
48. Ha, S.M., Wissler, M., Pelrine, R., Stanford S., Kovas, G., Pei, Q., Characterization of electroelastomers based on interpenetrating polymer networks, *Proc. SPIE*, 2007. 6524: 652408.
49. Plante, J.-S. and Dubowsky, S., On the performance mechanisms of dielectric elastomer actuators, *Sensors Actuators A*, 2007, 137: 96-109.

50. Zhao, X.H., Koh, S.J.A., Nonequilibrium thermodynamics of dielectric elastomers, submitted to *Int. J. Appl. Mech.*
51. Silberstein M.N. and Boyce, M.C., Constitutive modeling of the rate, temperature, and hydration dependent deformation response of Nafion to monotonic and cyclic loading, *J. Power Sources*, 2010, 195: 5692-5706.
52. Zhang, Q. M., Bharti, V. and Zhao, X., Giant electrostriction and relaxor ferroelectric behavior in electron-irradiated poly(vinylidene fluoride-trifluoroethylene) copolymer, *Science*, 1998, 280: 2101-2104.
53. Pelrine, R. E., Kornbluh, R. D. and Joseph, J. P., Electrostriction of polymer dielectrics with compliant electrodes as a means of actuation, *Sensors and Actuators A*, 1998, 64: 77-85.
54. Ha, S. M., Yuan, W., Pei, Q. B., Pelrine, R. and Stanford, S., Interpenetrating polymer networks for high-performance electroelastomer artificial muscles, *Adv. Mater.*, 2006, 18: 887-891 (2006).
55. Suo, Z.G., Zhu, J., Dielectric elastomers of interpenetrating networks, 2009, *Appl. Phys. Lett.*, 2009, 95: 232909.
56. Shankar, R., Ghosh, T. K. and Spontak, R. J., Electroactive nanostructured polymers as tunable actuators, *Adv. Mater.*, 2007, 19: 2218-2223.
57. Keplinger, C., Kaltenbrunner, M., Arnold, N. and Bauer, S., Röntgen's electrode-free elastomer actuators without electromechanical pull-in instability, *Proc. Nat. Acad. Sci.*, 2010, 107: 4505-4510.
58. Stark, K.H. and Garton, C.G., Electric strength of irradiated polythene. *Nature*, 1955, 176:1225–1226.
59. Zhao, X.H. and Suo, Z.G., Theory of dielectric elastomers capable of giant deformation of actuation, *Phys. Rev. Lett.*, 2010, 104: 178302.
60. Zhao X. H. and Suo, Z. G., Method to analyze electromechanical stability of dielectric elastomers, *Appl. Phys. Lett.*, 2007, 91: 061921.
61. Norris, A.N., Comments on “Method to analyze electromechanical stability of dielectric elastomers”, *Appl. Phys. Lett.*, 2008, 92: 026101.
62. Diaz-Calleja, R., Riande, E. and Sanchis, M.J., On electromechanical stability of dielectric elastomers, *Appl. Phys. Lett.*, 2008, 93: 101902.
63. Leng, J.S., Liu, L.W., Liu, Y.J., Yu, K., Sun, S.H., Electromechanical stability of dielectric elastomers, *Appl. Phys. Lett.*, 2009, 94: 211901.
64. Xu, B.-X., Mueller, R., Classen, M. and Gross, D., On electromechanical stability analysis of dielectric elastomer actuators, *Appl. Phys. Lett.*, 2010, 97: 162908.
65. Zhou, J.X., Hong, W., Zhao, X.H. and Suo, Z.G., Propagation of instability in dielectric elastomers, *Int. J. Solids Structures*, 2008, 45: 3739-3750.
66. Toupin, R.A., The elastic dielectric. *J. Rational Mech. Anal.* 1956, 5: 849-914.
67. Eringen, A.C., On the foundations of electroelastostatics. *Int. J. Engng. Sci.* 1963, 1: 127-153.
68. Tiersten, H.F., On the nonlinear equations of thermoelectroelasticity. *Int. J. Engng Sci.* 1971, 9: 587-604.
69. Vu, D. K., Steinmann, P. and Possart, G., Numerical modelling of non-linear electroelasticity, *Int. J. Numerical Methods Engng.*, 2007, 70, 685-704.
70. Zhao X. H. and Suo, Z. G., Method to analyze programmable deformation of dielectric elastomer layers, *Appl. Phys. Lett.*, 2008, 93: 251902.
71. O'Brien, B., McKay, T., Calius, E., Xie, S., I. Anderson, Finite element modelling of dielectric elastomer minimum energy structures, *Appl. Phys. A*, 2009, 94, 507-514.
72. Mockensturm, E.M. and Goulbourne, N., Dynamic response of dielectric elastomers, *Int. J. Non-Linear Mech.*, 2006, 41: 388-395.

73. Zhu, J., Stoyanov, H., Kofod, G. and Suo, Z.G., Large deformation and electromechanical instability of a dielectric elastomer tube actuator. *J. Appl. Phys.*, 2010, 108, 074113.
74. Zhu, J., Cai, S.Q., Suo, Z.G., Resonant behavior of a membrane of a dielectric elastomer. *Int. J. Solids Structures*, 2010, 47: 3254-3262.
75. Zhu, J., Cai, S.Q., Suo, Z.G., Nonlinear oscillation of a dielectric elastomer balloon, *Polymer International*, 2010, 59: 378-383 .
76. He, T.H., Zhao, X.H. and Suo, Z.G., Equilibrium and stability of dielectric elastomer membranes undergoing inhomogeneous deformation, *J. Appl. Phys.*, 2009, 106, 083522.

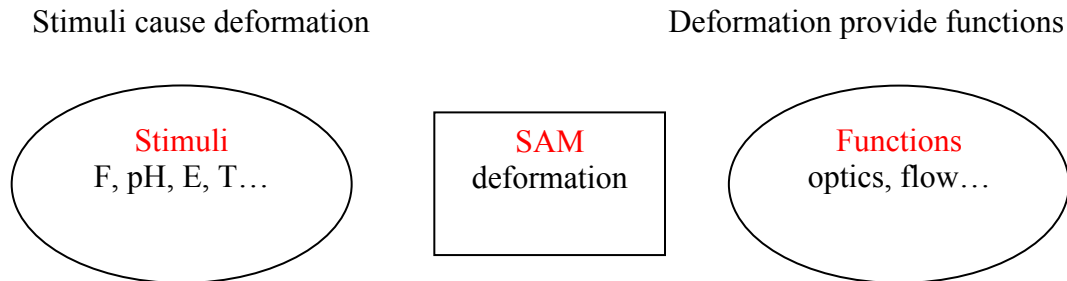
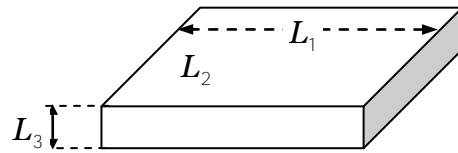


Fig.1. The environment affects a material through diverse stimuli, such as a force, an electric field, a change in pH, and a change in temperature. In response to a stimulus, a soft active material (SAM) deforms. The deformation provides a function, such as change in color and change in flow rate.

Reference state



Current state

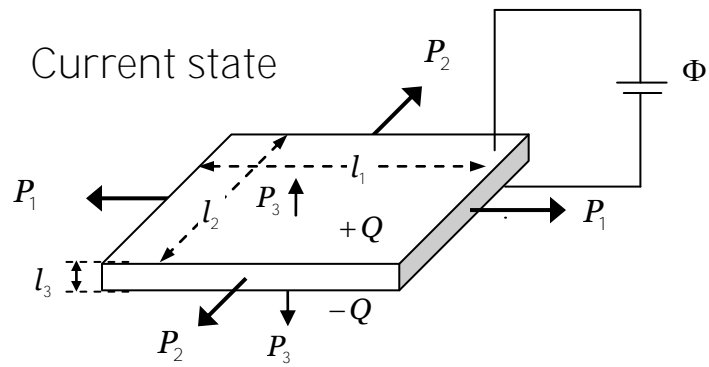


Fig. 2. A dielectric elastomer in the reference state and in a current state.

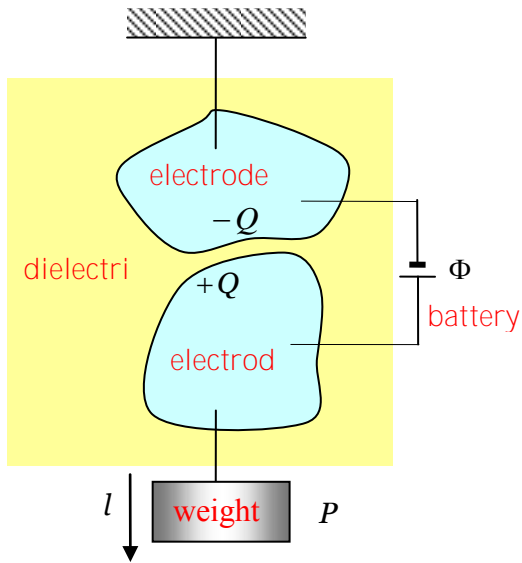


Fig.3. A transducer consists of a dielectric separating two electrodes. The transducer is subject to a force, represented by a weight P . The two electrodes are connected through a conducting wire to a battery of voltage Φ . The weight moves by distance l , and the battery pumps charge Q from one electrode to the other.

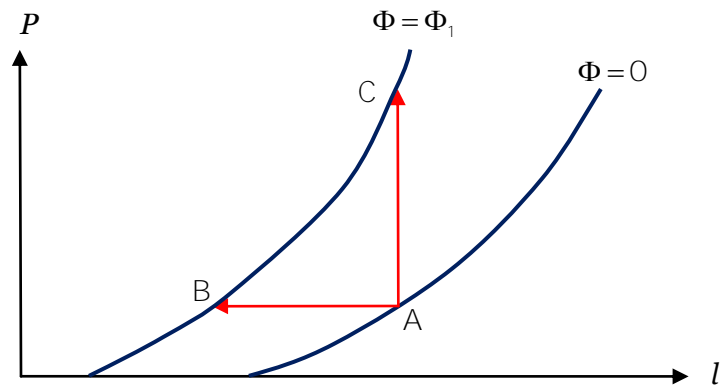


Fig. 4. In a plane with force and displacement as coordinates, a point represents a state of a transducer. A curve of a constant voltage is the force-displacement curve measured when the transducer is subject to a constant voltage.

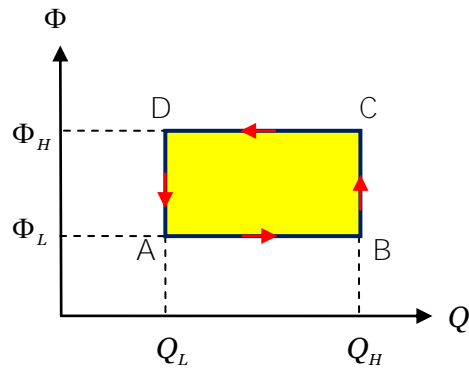


Fig. 5. In a plane with voltage and charge as coordinates, a point represents a state of a transducer. A use of the transducer typically involves a cyclic change of the state. The rectangle represents a cycle involving two levels of voltage and two values of charge.

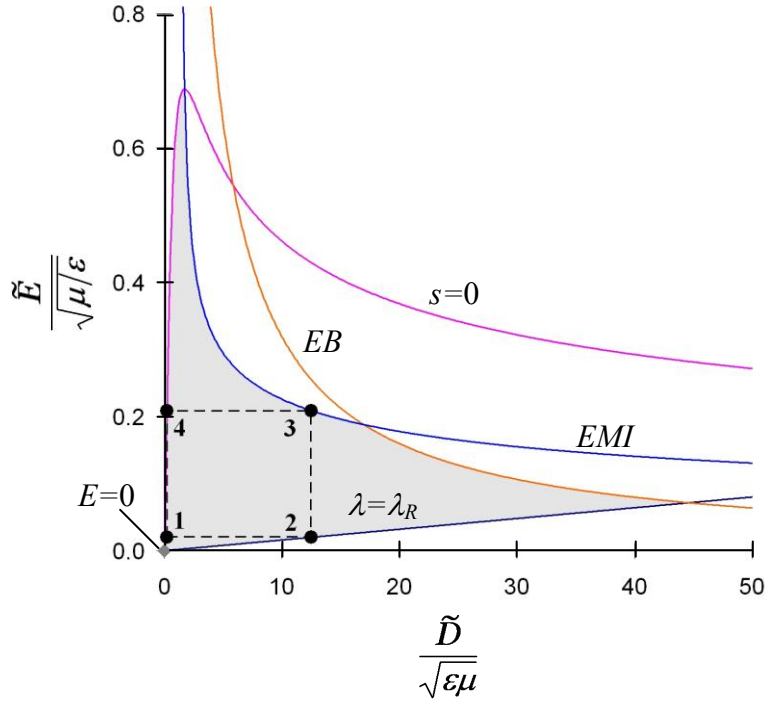


FIG. 6. A state of a dielectric membrane is represented by a point in the charge-voltage plane. The coordinates are given in dimensionless forms. Plotted are curves representing various modes of failure: electrical breakdown (**EB**), electromechanical instability (**EMI**), loss of tension ($s=0$), and rupture by stretch ($\lambda=\lambda_R$). These curves bound the region of allowable states of the transducer. A cycle involving two levels of voltage and two values of charge is represented by dotted lines.

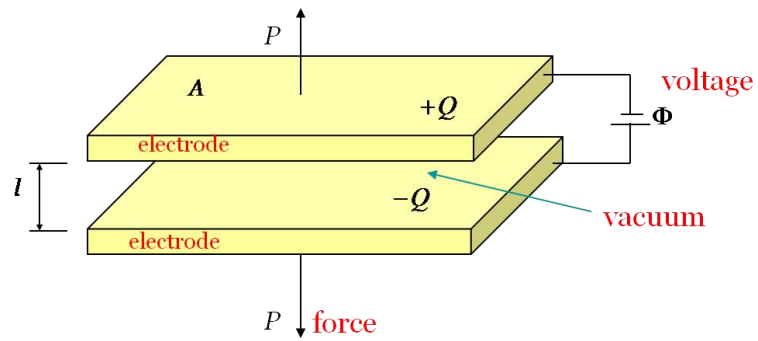


Fig. 7. A parallel-plate capacitor consists of two electrodes separated by a thin gap of a vacuum. When a voltage is applied, the two electrodes attract each other. The electrostatic attraction is balanced by applying a force.

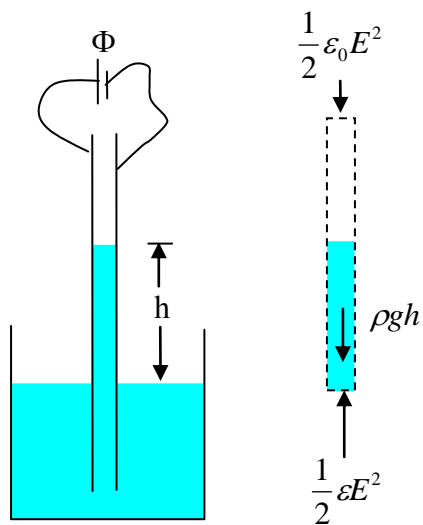


Fig. 8. A parallel-plate capacitor is partly in the air and partly in a liquid. When a voltage is applied, the liquid rises. As indicated by the free-body diagram on the right, the rise of the liquid is due to the balance between the Maxwell stress and the weight of the liquid.

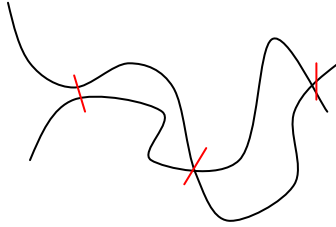


Fig. 9. An elastomer is a three dimensional network of long and flexible polymer chains. Each polymer chain consists of a large number of monomers.

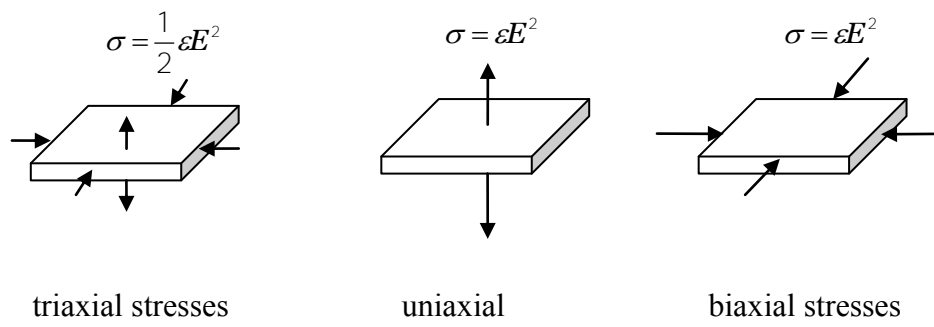


Fig.10. A dielectric in three states of stresses.

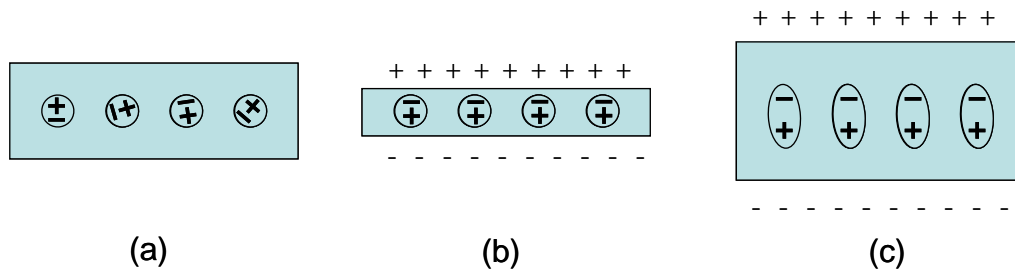


Fig. 11. Consider a dielectric that is nonpolar in the absence of applied voltage (a). Subject to a voltage, some dielectrics become thinner (b), but other dielectrics become thicker (c).

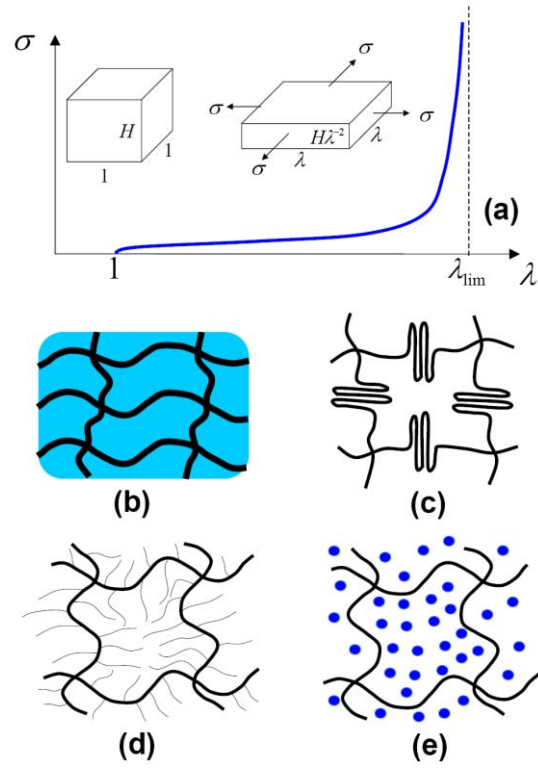


FIG. 12. (a) Stress-stretch curve of a membrane under biaxial stresses. (b) Fibers embedded in a compliant matrix. (c) A network of polymers with folded domains. (d) A network of polymers with side chains. (e) A network of polymers swollen with a solvent.

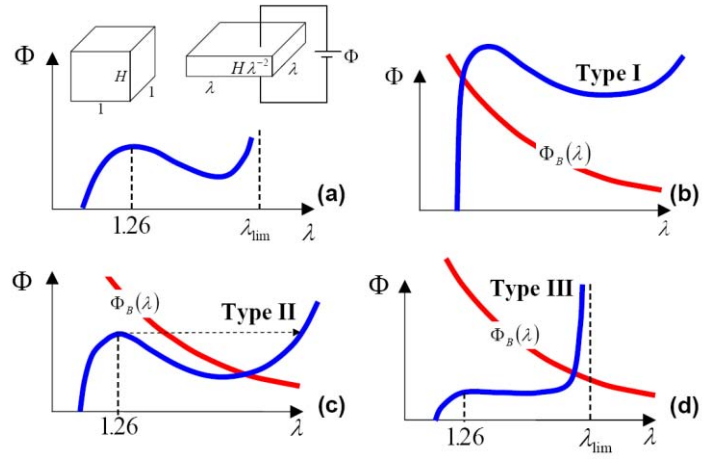


FIG. 13. (a) A membrane of a dielectric elastomer subject to a voltage reduces thickness and expands area. The voltage-stretch curve is typically not monotonic. (b-d) Three types behavior are distinguished, depending on where the two curves $\Phi(\lambda)$ and $\Phi_B(\lambda)$ intersect.

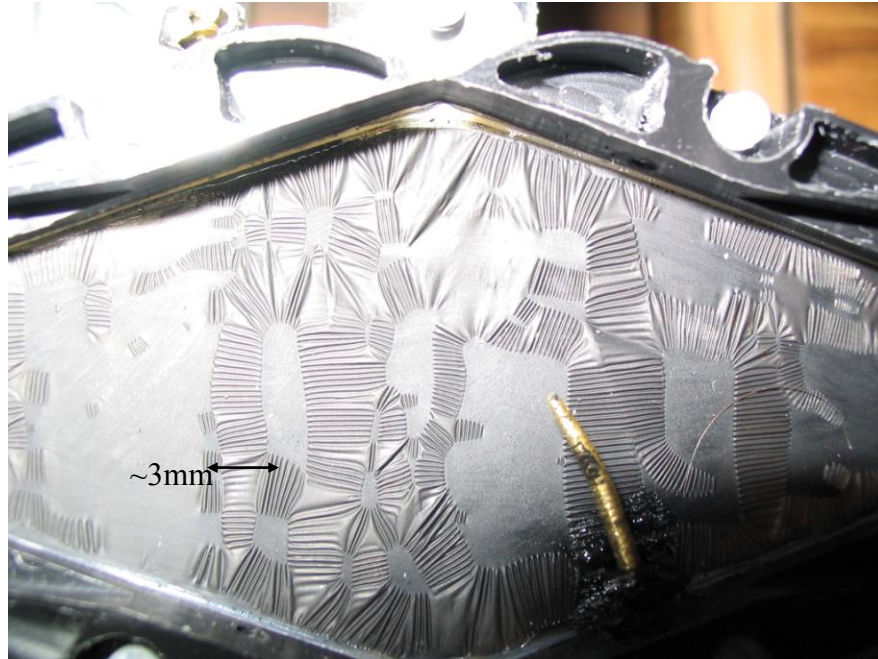


Fig. 14. An experimental observation of electromechanical instability (courtesy of JS Plante and S Dubowsky). A layer of a dielectric elastomer, coated with conductive grease on top and bottom faces, is pre-stretched using a frame. An electric voltage is applied between the two electrodes. The layer deforms into a mixture of two regions, one being flat and the other wrinkled.